Scott, J.C., Stefaniak, J., Pawlowski, Z.S., McManus, D.P., 1997. Molecular genetic analysis of human cystic hydatid cases from Poland: identification of a new genotypic group (G9) of *Echinococcus granulosus*. Parasitology 114, 37–43.

Sinha, S., Sharma, B.S., 2009. Neurocysticercosis: a review of current status and management. J. Clin. Neurosci. 16, 867–876.

Stefanić, S., Shaikenov, B.S., Deplazes, P., Dinkel, A., Torgerson, P.R., Mathis, A., 2004. Polymerase chain reaction for detection of patent infections of *Echinococcus granulosus* ("sheep strain") in naturally infected dogs. Parasitol. Res. 92, 347–351.

Tang, C., Cui, G., Qian, Y., Kang, Y., Wang, Y., Peng, W., Lu, H., Chen, D., 2007. Studies on the alveolar *Echinococcus* species in northward Daxingan mountains, Inner Mongolia, China. III. *Echinococcus russicensis* sp. nov. Chin. J. Zoonoses 23, 957–963.

Thompson, R.C.A., 2008. The taxonomy, phylogeny and transmission of *Echinococcus*. Exp. Parasitol. 119, 439–446.

Thompson, R.C.A., McManus, D.P., 2002. Towards a taxonomic revision of the genus *Echinococcus*. Trends Parasitol. 18, 452–457.

Thompson, R.C.A., Lymbery, A.J., Constantine, C.C., 1995. Variation in *Echinococcus*: towards a taxonomic revision of the genus. Adv. Parasitol. 35, 145–176.

Tibayrenc, M., 2006. The species concept in parasites and other pathogens: a pragmatic approach? Trends Parasitol. 22, 66–70.

Torgerson, P.R., Deplazes, P., 2009. Echinococcosis: diagnosis and diagnostic interpretation in population studies. Trends Parasitol. 25, 164–170.

Trachsel, D., Deplazes, P., Mathis, A., 2007. Identification of taeniid eggs in the faeces from carnivores based on multiplex PCR using targets in mitochondrial DNA. Parasitology 134, 911–920.

Vega, R., Piñero, D., Ramanankandrasana, B., Dumas, M., Bouteille, B., Fleury, A., Sciutto, E., Larralde, C., Fragoso, G., 2003. Population genetic structure of *Taenia solium* from Madagascar and Mexico: implications for clinical profile diversity and immunological technology. Int. J. Parasitol. 33, 1479–1485.

Verster, A., 1965. Review of *Echinococcus* species in South Africa. Onderstepoort J. Vet. Res. 32, 7–118.

Verster, A., 1969. A taxonomic revision of the genus *Taenia* Linnaeus, 1758s. str. Onderstepoort J. Vet. Res. 36, 3–58.

Vogel, H., 1957. Ueber den *Echinococcus multilocularis* Süddeutschlands. I. Das Bandwurmstadium von Stämmen menschlicher und tierischer Herkunft. Z. Tropenmed. Parasitology 8, 404–454.

von Nickisch-Rosenegk, M., Silva-Gonzalez, R., Lucius, R., 1999. Modification of universal 12S rDNA primers for specific amplification of contaminated *Taenia* spp. (Cestoda) gDNA enabling phylogenetic studies. Parasitol. Res. 85, 819–825.

Williams, R.J., Sweatman, G.K., 1963. On the transmission, biology and morphology of *Echinococcus granulosus equinus*, a new subspecies of hydatid tapeworm in horses in Great Britain. Parasitology 53, 391–407.

Xiao, N., Qiu, J., Nakao, M., Li, T., Yang, W., Chen, X., Schantz, P.M., Craig, P.S., Ito, A., 2005. *Echinococcus shiquicus* n. sp., a taeniid cestode from Tibetan fox and plateau pika in China. Int. J. Parasitol. 35, 693–701.

Yamasaki, H., Allan, J.C., Sato, M.O., Nakao, M., Sako, Y., Nakaya, K., Qiu, D., Mamuti, W., Craig, P.S., Ito, A., 2004a. DNA differential diagnosis of taeniasis and cysticercosis by multiplex PCR. J. Clin. Microbiol. 42, 548–553.

Yamasaki, H., Matsunaga, S., Yamamura, K., Chang, C.C., Kawamura, S., Sako, Y., Nakao, M., Nakaya, K., Ito, A., 2004b. Solitary neurocysticercosis case caused by Asian genotype of *Taenia solium* confirmed by mitochondrial DNA analysis. J. Clin. Microbiol. 42, 3891–3893.

Yamasaki, H., Nakao, M., Nakaya, K., Schantz, P.M., Ito, A., 2008. Genetic analysis of *Echinococcus multilocularis* originating from a patient with alveolar echinococcosis occurring in Minnesota in 1977. Am. J. Trop. Med. Hyg. 79, 245–247.

Yamasaki, H., Nakao, M., Sako, Y., Nakaya, K., Sato, M.O., Mamuti, W., Okamoto, M., Ito, A., 2002. DNA differential diagnosis of human taeniid cestodes by base excision sequence scanning thymine-base reader analysis with mitochondrial genes. J. Clin. Microbiol. 40, 3818–3821.

Yanagida, T., Yuzawa, I., Joshi, D.D., Sako, Y., Nakao, M., Nakaya, K., Kawano, N., Oka, H., Fujii, K., Ito, A., in press. Neurocysticercosis: assessing where the infection was acquired? J. Travel Med.

Yang, Y.R., Rosenzvit, M.C., Zhang, L.H., Zhang, J.Z., McManus, D.P., 2005. Molecular study of *Echinococcus* in west-central China. Parasitology 131, 547–555.

Zhang, L., Gasser, R.B., Zhu, X., McManus, D.P., 1999. Screening for different genotypes of *Echinococcus granulosus* within China and Argentina by single-strand conformation polymorphism (SSCP) analysis. Trans. R. Soc. Trop. Med. Hyg. 93, 329–334.

Zhang, L., Hu, M., Jones, A., Allsopp, B.A., Beveridge, I., Schindler, A.R., Gasser, R.B., 2007. Characterization of *Taenia madoquae* and *Taenia regis* from carnivores in Kenya using genetic markers in nuclear and mitochondrial DNA, and their relationships with other selected taeniids. Mol. Cell. Probes 21, 379–385.

CLINICAL AND VACCINE IMMUNOLOGY, June 2010, p. 944–948 Vol. 17, No. 6
1556-6811/10/$12.00 doi:10.1128/CVI.00026-10

Immunoglobulin G Subclass Responses to Recombinant Em18 in the Follow-Up of Patients with Alveolar Echinococcosis in Different Clinical Stages[▽]

Dennis Tappe,[1]*§ Yasuhito Sako,[2]§ Sonoyo Itoh,[2] Matthias Frosch,[1] Beate Grüner,[3] Peter Kern,[3] and Akira Ito[2]§

Institute of Hygiene and Microbiology, Josef-Schneider-Str. 2, 97080 Würzburg,[1] and Comprehensive Infectious Diseases Center, Division of Infectious Diseases and Clinical Immunology, University Hospital and Medical Center Ulm, Albert-Einstein-Allee 23, 89081 Ulm,[3] Germany, and Department of Parasitology, Asahikawa Medical College, Midorigaoka Higashi 2-1-1-1, Asahikawa 078-8510, Japan[2]

Received 13 January 2010/Returned for modification 15 March 2010/Accepted 2 April 2010

In this study, we compared the sequential responses of immunoglobulin G (IgG) subclasses to the diagnostic antigen Em18 in sera from patients with alveolar echinococcosis. A total of 225 sera from 36 patients at different clinical stages according to the WHO-PNM staging system were tested. The antibody responses were measured for cohorts with resected and unresected parasitic lesions by enzyme-linked immunosorbent assays (ELISA). Total IgG and, to a lesser extent, IgG4 antibody levels against Em18 correlated with all PNM stages before treatment, whereas levels of IgG2 were low and IgG3 was undetectable. Antibody kinetics, however, depended on the treatment rather than on the PNM stage. For some patients, after curative surgery, IgG1 antibodies dropped below the cutoff earlier than other antibodies, followed by total IgG and IgG4 within 18 months. For some patients with recurrences after surgery, IgG1 and IgG4 reappeared, whereas patients with unresectable lesions but stable disease showed steady declines in the levels of all antibodies, and IgG1 became undetectable in some patients. Additional testing of IgE responses to Em18 showed constantly low levels at all stages and in all cohorts.

Alveolar echinococcosis (AE) is caused by the vesicular larval stage of the fox tapeworm *Echinococcus multilocularis*. The helminth causes dangerous infections characterized by infiltrative growth of the larvae in the livers of natural intermediate hosts such as rodents, and rarely in humans. Metastasis formation may also occur. AE is staged according to the World Health Organization (WHO)-PNM (P, parasitic mass in the liver; N, involvement of neighboring organs; M, metastasis) system (10). Radical resection of parasitic lesions is the preferred treatment (1), but most patients are inoperable at the time of diagnosis (5, 13). In a recent serological study, immunoglobulin G (IgG) antibodies directed against Em18, Em10, and Em2plus antigen compositions showed a close relationship between the clinical status and the treatment of patients with AE (16). In direct comparison, antibodies against Em18 demonstrated the greatest dynamic changeability in all patients, cohorts, and PNM stages, irrespective of the individual treatment. Moreover, Em18 indices had shown the best correlation with the PNM stages prior to treatment. These results prompted us to further investigate the IgG subclass and additionally the IgE response against this diagnostic antigen in patients with either resected or unresectable parasitic lesions.

* Corresponding author. Mailing address: Institute of Hygiene and Microbiology, Josef-Schneider-Str. 2, 97080 Würzburg, Germany. Phone: 49-931-201-46036. Fax: 49-931-201-46445. E-mail: dtappe@hygiene.uni-wuerzburg.de.

§ D.T., Y.S., and A.I. contributed equally to this work.

▽ Published ahead of print on 14 April 2010.

MATERIALS AND METHODS

Patients. All patients described in this study were seen at the University Hospital and Medical Center Ulm, Ulm, Germany. A total of 36 patients (225 sera) with a history of hepatic AE and a follow-up period of 1.5 to 6.5 years were included in the study. The patients (age range, 17 to 86 years; mean age, 51.2 years; sex ratio [male to female], 0.57:1) were assigned to different clinical WHO-PNM stages of the disease. All patients had acquired AE in Germany and received benzimidazole therapy. Thirteen patients had curatively resected lesions; 4 had recurrences after surgery; 1 had a palliative resection only; 16 had unresectable lesions but stable disease; and 2 had apparently dead, fully calcified lesions (Table 1). All serum samples were tested at the Department of Parasitology, Asahikawa Medical College, Asahikawa, Japan, in a blind test. The classification of curative resection, stable disease, progressive disease, or the presence of an apparently dead, fully calcified lesion was established by magnetic resonance imaging based on lesion size and morphology at the respective follow-up intervals. Ethical approval was obtained from the University of Ulm.

Methods. For the Em18 enzyme-linked immunosorbent assay (ELISA), recombinant Em18 antigen (14) was used to coat microtiter plates at a concentration of 100 ng/well. Patients' sera were tested at dilutions of 1:100 for total IgG and IgG subclasses, and 1:10 for IgE, after preabsorption of the wells with 1% casein in 20 mM Tris-HCl (pH 7.4)–150 mM NaCl buffer. Serum IgG bound to echinococcal antigens were detected with horseradish peroxidase (HRP)-conjugated protein G (Zymed) as a secondary antibody by using 2,2′-azinobis(3-ethylbenzthiazolinesulfonic acid) (ABTS; Sigma, Germany) as a chromogenic substrate. For the detection of recombinant Em18-specific IgE and IgG subclasses, HRP-conjugated mouse monoclonal anti-human IgE, IgG1, IgG2, IgG3, or IgG4 antibodies (Zymed) were used. Absorbance was measured after 30 min at 405 nm with a reference wavelength of 630 nm. For the calculation of the cutoff, the mean value of the absorbances of 31 sera from healthy blood donors was added to 3 times the standard deviation (SD) for total IgG and to 5 times the SD for the IgG subclasses and IgE. The index of the individual serum sample was calculated by dividing the sample's absorbance by the cutoff.

Statistical analysis. Statistical analyses were performed with the free software environment "R" for statistical computing. Nonparametric data were analyzed using Spearman's rank test for the correlation of the clinical stage and the ELISA

TABLE 1. Characteristics of patients with alveolar echinococcosis included in the study

Patient no.	Stage	PNM code[a]	Status[a]	Age (yr)[b]	Sex	Follow-up duration (yr)
1	I	P1N0M0	Curative resection	62	F	5.5
2	I	P1N0M0	Curative resection	24	F	5
3	I	P1N0M0	Curative resection	22	F	4
4	I	P1N0M0	Curative resection	33	F	2
5	I	P1N0M0	Apparently dead, fully calcified lesion	58	M	4
6	I	P1N0M0	Unresectable, stable disease	61	M	3.5
7	II	P2N0M0	Curative resection	38	F	3
8	II	P2N0M0	Unresectable, stable disease	71	M	6
9	II	P2N0M0	Unresectable, stable disease	68	F	5.5
10	II	P2N0M0	Unresectable, stable disease	59	F	6.5
11	II	P2N0M0	Unresectable, stable disease	60	F	6
12	II	P2N0M0	Curative resection	41	F	2.5
13	II	P2N0M0	Recurrence after resection	74	F	2.5
14	II	P2N0M0	Unresectable, stable disease	75	M	3
15	IIIa	P3N0M0	Curative resection	25	F	4.5
16	IIIa	P3N0M0	Curative resection	62	M	5.5
17	IIIa	P3N0M0	Recurrence after resection	17	F	3.5
18	IIIa	P3N0M0	Unresectable, stable disease	69	F	6
19	IIIa	P3N0M0	Unresectable, stable disease	39	F	4
20	IIIa	P3N0M0	Apparently dead, fully calcified lesion	57	F	6
21	IIIa	P3N0M0	Unresectable, stable disease	43	M	2
22	IIIa	P3N0M0	Recurrence after resection	19	F	3
23	IIIb	P4N0M0	Unresectable, stable disease	60	F	5
24	IIIb	P3N1M0	Unresectable, stable disease	49	F	5.5
25	IIIb	P2N1M0	Recurrence after resection	50	M	5
26	IIIb	P3N1M0	Progression after palliative resection	32	M	6
27	IIIb	P4N0M0	Unresectable, stable disease	57	M	3
28	IIIb	P4N0M0	Unresectable, stable disease	86	F	5.5
29	IV	P4N1M0	Curative resection	56	F	6.5
30	IV	P4N1M0	Curative resection	30	M	3
31	IV	P4N1M0	Curative resection	72	F	3
32	IV	P4N1M0	Unresectable, stable disease	71	F	5.5
33	IV	P4N1M0	Curative resection	52	M	2.5
34	IV	P4N1M0	Curative resection	63	F	1.5
35	IV	P4N1M0	Unresectable, stable disease	34	M	2.5
36	IV	P4N1M0	Unresectable, stable disease	54	M	4

[a] As assessed either by imaging alone (apparently dead lesion, progressive disease, and stable disease) or by imaging and histology (curative resection).
[b] At the time when the first blood sample was drawn.

index of the respective antibody (subclass) responses. P values of <0.005 were regarded as significant.

RESULTS

The height of the ELISA index of the antibodies tested showed a weak correlation of total IgG and IgG4 with all clinical PNM stages (stages I to IV) prior to treatment (Fig. 1a). IgG4 showed a close-to-linear correlation only with the first three stages (stages I to IIIa). The correlation of IgG1 was poor. Since IgE and IgG2 antibodies showed weak reactivities, and IgG3 antibodies were undetectable, no correlation with the clinical stage could be established for these isotypes/subclasses at all. The clinical PNM stage had no influence on the kinetics of antibody levels *per se*. Rather, antibody levels depended on the treatment the patients underwent at each stage (Fig. 1b and c).

In the cohort of 13 patients who underwent curative resection, levels of all antibodies decreased rapidly after resection of the parasitic lesions. Antibody levels dropped below the cutoff level after some time (Fig. 1b). The index of IgG4 directed against Em18 showed the most marked decline of all antibody (sub)types during the first follow-up interval in all patients and PNM stages in this cohort (Fig. 1b). IgG1 antibodies were the first to drop below the cutoff in some patients, followed by total IgG and IgG4. IgG1 fell below the cutoff in 8 patients (patients 2, 7, 12, 15, 16, 29, 33, and 34) after 30, 12, 24, 6, 12, 12, 6, and 6 months, respectively; total IgG fell below the cutoff in 6 patients (patients 2, 7, 12, 15, 29, and 34) at 54, 12, 24, 6, 12, and 18 months, respectively; and IgG4 fell below the cutoff in 6 patients (patients 2, 7, 12, 15, 29, and 34) after 30, 12, 24, 6, 48, and 18 months, respectively. In some patients, seroreversion in different assays was seen at the same time. Once seroreversion was seen, antibodies remained undetectable throughout the observation period. Follow-up imaging demonstrated that the drop below the cutoff level reflected serologically the clinical regression in this patient cohort.

In the 5 patients with noncurative resection, antibody levels of total IgG, IgG1, and IgG4 against Em18 decreased at first but increased again during the follow-up period. Total IgG never fell below the cutoff level, whereas IgG1 became negative in 2 patients (patients 22 and 26) after 6 and 36 months and increased again after 24 and 54 months, respectively. IgG4 became negative in 1 patient (patient 22) and showed the same kinetics as IgG1 in this patient. Re-

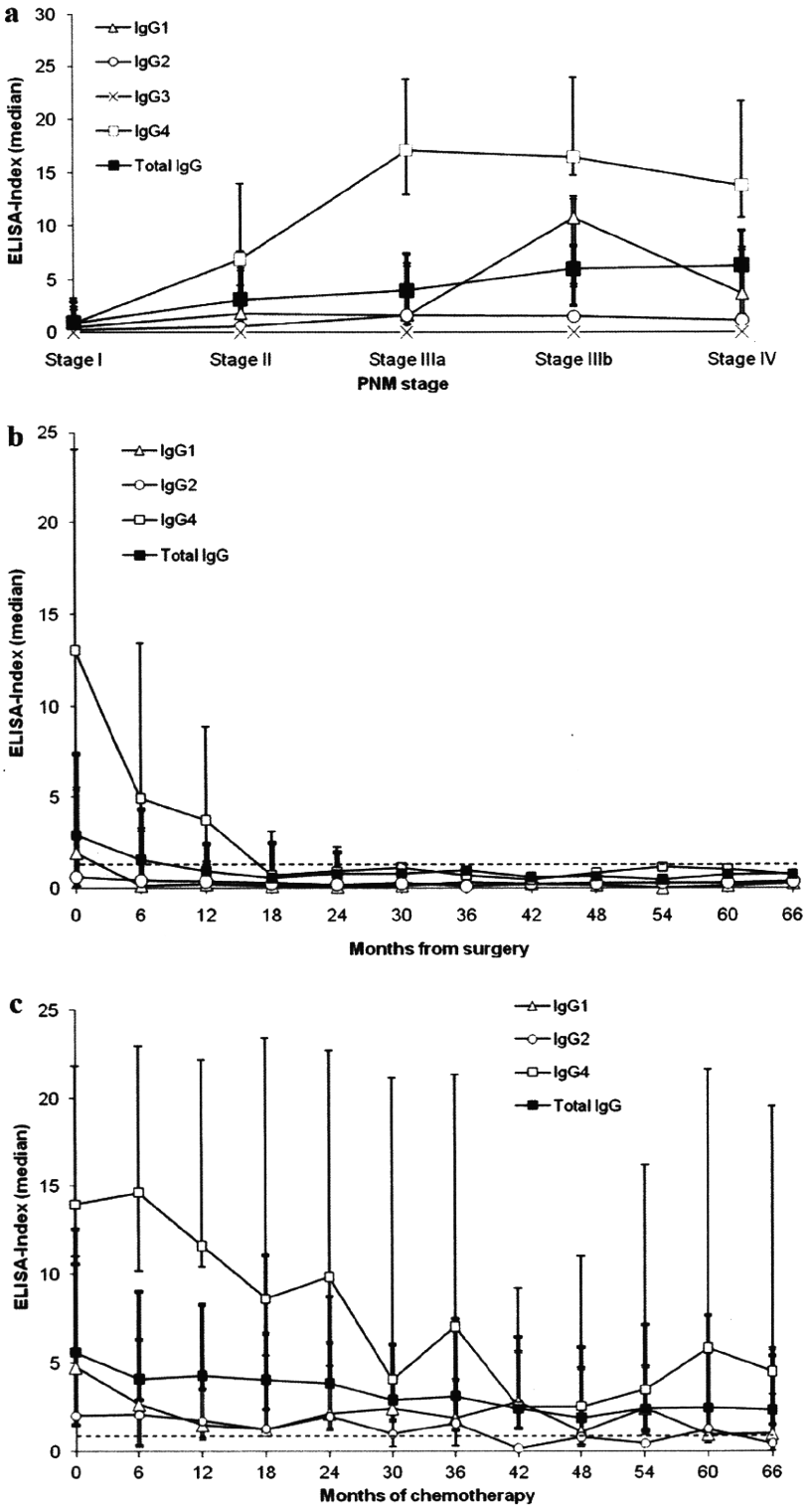

FIG. 1. (a) Correlation of the PNM stage and the ELISA-index prior to treatment. Median index values of the respective antibodies against Em18 are displayed for each PNM stage. The highest median index in all stages was demonstrated for IgG4, whereas IgG3 was completely unreactive. The lowest positive median indices in all stages were demonstrated for IgE (data not shown) and IgG2. A constant increase in the median values of the total IgG index in parallel with the clinical stage is visible. IgG4 indices showed a close-to-linear increase for stages I to IIIa only. Error bars represent ranges for total IgG (bold lines), IgG4 (thin single lines), and IgG1 (thin double lines). Spearman's rank correlation coefficients (ρ) for total IgG, IgG4, and IgG1 with all PNM stages (stages I to IV) were 0.532 (P, <0.001), 0.499 (P, <0.002), and 0.358 (P, <0.05),

currence was demonstrated by follow-up imaging in all patients.

In the cohort of 16 patients with unresectable lesions and stable disease under benzimidazole therapy, total-IgG, IgG1, IgG2, and IgG4 levels showed slow but steady declines (Fig. 1c). IgE levels were very low. No differences in antibody kinetics between different PNM stages in this patient cohort were observed. Overall, the IgG4 index demonstrated the most pronounced decrease in all patients and PNM stages of this cohort. Total IgG showed the smoothest decline, whereas IgG1 and IgG4 displayed undulating decreases. IgG1, IgG2, and IgG4 antibodies dropped below the cutoff in 5 patients (patients 8, 10, 11, 18, and 19) after 12, 36, 72, 18, and 42 months, respectively; in 2 patients (patients 11 and 32) after 12 and 42 months, respectively; and in 1 patient (patient 11) after 72 months. Once seroreversion was seen, antibodies remained undetectable throughout the observation period. The decrease in the antibody levels paralleled serologically the clinically stable disease in this patient cohort as assessed by follow-up imaging.

In the 2 patients with apparently dead lesions, levels of all antibodies against Em18 either were completely below the cutoff or showed a steady decline until total IgG, IgG1, and IgG4 became undetectable at the same time (data not shown). The apparently dead, fully calcified lesions correlated with no detectable growth during follow-up imaging. Testing of IgE responses to Em18 showed constantly low levels in all stages and cohorts (data not shown).

DISCUSSION

In this study, we performed a serological follow-up of patients with AE grouped according to the WHO-PNM staging system. The recombinant diagnostic antigen Em18 was used in different ELISAs, which measured total IgG, IgG subclasses, and IgE in a German patient cohort. Six different assays were run in parallel. In a previous study, the height of antibody levels prior to treatment was dependent on the PNM stage, and indices of anti-Em18 IgG showed the highest correlation of all antigen compositions used (16). Here, a similar correlation was shown for total IgG against Em18. When the IgG subclass responses were analyzed, however, only IgG4 displayed a comparable correlation with all clinical PNM stages before treatment was begun. IgG4 also exhibited the highest ELISA indices in all patient subcohorts and stages, suggesting a higher diagnostic sensitivity than those for other subclasses or total IgG (7). Accordingly, earlier studies have shown that IgG4 was the predominant IgG subclass responding to Em18 (8). In another study, IgG4 and IgG1 isotype levels were significantly elevated in the sera of AE patients (18), and these isotypes also displayed the most sensitive antibody response to a crude parasite extract containing a 17.5- to 18-kDa antigen in an ELISA (18) and immunoblot analysis (4, 20). In our study, IgG1 levels against Em18 were also increased at all clinical stages, whereas IgG2 demonstrated the lowest positive median indices at all stages, and IgG3 was completely undetectable. Since Em18 is a pure protein antigen, and IgG2 has often been associated with anticarbohydrate immune responses in humans (17), it is understandable that only a low IgG2 response was obtained. Why IgG3 was undetectable in our study is less clear. A greater-than-expected proportion of carbohydrate-specific IgG antibody responses in humans can have a non-IgG2 subclass origin (17), possibly also encompassing IgG3. Hypothetically, a suppression of IgG3 responses toward this diagnostic antigen by the parasite might also be possible. In a previous study by others, the sensitivities of IgG2 and IgG3 directed against a crude parasite extract were also significantly lower than those of the other IgG subclasses in AE patients (19). Levels of IgE in response to Em18 were very low in all stages and patient cohorts. These data indicate that Em18 is a good candidate for parasite-specific total-IgG, IgG4, and IgG1 analysis of AE patients at all WHO stages. Em18 might be an unsuitable antigen for IgE and IgG2 testing, and an unsuitable antigen as a pure protein for IgG3 serology as well.

In the follow-up investigations, IgG4 antibodies against Em18 demonstrated the greatest dynamic changeability in all patients, cohorts, and PNM stages, irrespective of the individual treatment. The data obtained from the patient cohort with curatively resected lesions are consistent with previous findings that antibodies directed against various antigen compositions, including Em18, can drop below the cutoff (2, 6, 15, 16). In this study, IgG1 antibodies were the first to drop below the cutoff, followed by total IgG and IgG4 at 6-month intervals, reflecting the curative resection. In contrast, in a previous follow-up study of cured or improved patients, levels of IgG4 antibodies directed against a crude parasite extract tended to decrease earlier than total-IgG levels (18). However, IgG4 antibodies became negative 1 year after successful treatment, as seen in our study.

For patients with recurrences, the initial decrease in the levels of total IgG against Em18, followed by a later increase, has previously been demonstrated in other studies using total IgG in the Em18 ELISA (6, 16), Em18 Western blotting (12), and other assays with different diagnostic antigens (16). Levels of IgG1 and IgG4 against Em18 followed these kinetics, but these antibodies became intermittently negative in a few patients in this study. Accordingly, specific IgG4 responses to a crude antigen extract reappeared in recurrences, as shown in a survey by others (18).

respectively. (b) Antibody profiles of patients after curative resection. Median index values from all assays (except those for IgG3 and IgE) for 13 patients at different clinical stages are presented. Rapid declines in the antibody indices of total IgG, IgG1, and IgG4 are clearly visible. Error bars represent ranges (until month 24) for total IgG, IgG4, and IgG1 as explained for panel a. Serological data were accumulated for intervals of 6 months. At each given interval, data from 2 to 13 patients were available. The cutoff level is 1, represented by the dashed line. The time of resection is month zero. (c) Antibody profiles of patients with stable disease and unresectable lesions. Median index values from all assays (except those for IgG3 and IgE) for 16 patients at different clinical stages are presented. A slow decline in the antibody indices is visible. Error bars represent ranges for total IgG, IgG4, and IgG1 as explained for panel a. Serological data were accumulated for intervals of 6 months. At each given interval, data from 5 to 16 patients were available. The cutoff level is 1, represented by the dashed line. The start of chemotherapy is at month zero.

Our results for the patient cohort with unresectable lesions and stable AE are consistent with previous findings that levels of antibody against Em18 (6, 12, 16), and also other diagnostic antigens (2, 12, 16), decrease slowly under antiparasitic chemotherapy. In our study, total IgG against Em18 showed the smoothest decline, whereas median indices of IgG1 and IgG4 demonstrated undulating decreases over time. In a previous study by others, levels of IgG1 and IgG4 against Em18 fell to zero in some patients treated with albendazole (12), whereas these IgG subclasses showed unchanged levels against a crude parasite antigen extract in patients with stabilized AE (18). In our study, seroreversion was also demonstrable for IgG1 in some patients and for IgG2 and IgG4 in a few patients. Most patients were at an early stage of the disease (stage II). In this patient group, a regression of lesions toward nonviability of the parasite might be possible. However, the observation period might not have been long enough to demonstrate seroreversion in the other IgG subclasses or total IgG.

The kinetics of antibody levels in patients who have apparently dead and fully calcified lesions were very similar to those for the cohort with stable disease, and the results are consistent with those of a previous report (16).

Whether the IgG subclass effect described here is directly related to the Em18 antigen or is a more general effect of AE serology remains to be elucidated. However, several previous studies found that the recombinant Em18 antigen may be one of the best antigens for AE serology (3, 9, 11, 14, 16). Antibody responses to recombinant proteins are much clearer, and thus easier to analyze, than responses to native proteins, since the latter may contain variable epitopes, which may lead to more complex immunological responses.

In conclusion, our data indicate that the diagnostic antigen Em18 is suitable for parasite-specific serology employing total-IgG, IgG1, and IgG4 assays. Total IgG and IgG4 mirror the clinical PNM stage best before treatment. IgG4 shows the greatest changes in all patient cohorts, clinical stages, and treatments; therefore, IgG4 might be the most sensitive antibody subclass for AE serology employing the Em18 antigen. IgG1 antibody kinetics reflect curative resection, recurrence, and possibly the death of the parasite better than any other antibody (sub)class directed against Em18.

ACKNOWLEDGMENTS

We thank Christoph Schoen (Germany) for assistance with the statistical analysis.

Serology in Japan was financially supported in part by the Infection Matrix Fund (2007 to 2008) and the Hokkaido Translational Research Project (2007 to 2012) from the Ministry of Education, Japan, and by the Japan Society for the Promotion of Science (21256003) (to A.I.).

REFERENCES

1. **Ammann, R. W., and J. Eckert.** 1996. Cestodes. *Echinococcus.* Gastroenterol. Clin. North Am. **25:**655–689.
2. **Ammann, R. W., E. C. Renner, B. Gottstein, F. Grimm, J. Eckert, and E. L. Renner; Swiss Echinococcosis Study Group.** 2004. Immunosurveillance of alveolar echinococcosis by specific humoral and cellular immune tests: long-term analysis of the Swiss chemotherapy trial (1976–2001). J. Hepatol. **41:** 551–559.
3. **Bart, J. M., M. Piarroux, Y. Sako, F. Grenouillet, S. Bresson-Hadni, R. Piarroux, and A. Ito.** 2007. Comparison of several commercial serologic kits and Em18 serology for detection of human alveolar echinococcosis. Diagn. Microbiol. Infect. Dis. **59:**93–95.
4. **Dreweck, C. M., C. G. Lüder, P. T. Soboslay, and P. Kern.** 1997. Subclass-specific serological reactivity and IgG4-specific antigen recognition in human echinococcosis. Trop. Med. Int. Health **2:**779–787.
5. **Eckert, J., P. Jacquier, D. Baumann, and P. A. Raeber.** 1995. Echinokokkose des Menschen in der Schweiz, 1984–1992. Schweiz. Med. Wochenschr. **125:** 1989–1998.
6. **Fujimoto, Y., A. Ito, Y. Ishikawa, M. Inoue, Y. Suzuki, M. Ohhira, T. Ohtake, and Y. Kohgo.** 2005. Usefulness of recombinant Em18-ELISA to evaluate efficacy of treatment in patients with alveolar echinococcosis. J. Gastroenterol. **40:**426–431.
7. **Ishikawa, Y., Y. Sako, S. Itoh, T. Ohtake, Y. Kohgo, T. Matuno, Y. Ohsaki, N. Miyokawa, M. Nakao, K. Nakaya, and A. Ito.** 2009. Serological monitoring of progression of alveolar echinococcosis with multiorgan involvement by use of recombinant Em18. J. Clin. Microbiol. **47:**3191–3196.
8. **Ito, A., P. M. Schantz, and J. F. Wilson.** 1995. Em18, a new serodiagnostic marker for differentiation of active and inactive cases of alveolar hydatid disease. Am. J. Trop. Med. Hyg. **52:**41–44.
9. **Ito, A., N. Xiao, M. Liance, M. O. Sato, Y. Sako, W. Mamuti, Y. Ishikawa, M. Nakao, H. Yamasaki, K. Nakaya, K. Bardonnet, S. Bresson-Hadni, and D. A. Vuitton.** 2002. Evaluation of an enzyme-linked immunosorbent assay (ELISA) with affinity-purified Em18 and an ELISA with recombinant Em18 for differential diagnosis of alveolar echinococcosis: results of a blind test. J. Clin. Microbiol. **40:**4161–4165.
10. **Kern, P., H. Wen, N. Sato, D. A. Vuitton, B. Grüner, Y. Shao, E. Delabrousse, W. Kratzer, and S. Bresson-Hadni.** 2006. WHO classification of alveolar echinococcosis: principles and application. Parasitol. Int. **55:**S283–S287.
11. **Li, T., A. Ito, X. Chen, Y. Sako, J. Qiu, N. Xiao, D. Qiu, M. Nakao, T. Yanagida, and P. S. Craig.** 2010. Specific IgG responses to recombinant antigen B and Em18 in cystic and alveolar echinococcosis in China. Clin. Vaccine Immunol. **17:**470–475.
12. **Ma, L., A. Ito, Y. H. Liu, X. G. Wang, Y. G. Yao, D. G. Yu, and Y. T. Chen.** 1997. Alveolar echinococcosis: Em2 plus-ELISA and Em18-Western blots for follow-up after treatment with albendazole. Trans. R. Soc. Trop. Med. Hyg. **91:**476–478.
13. **Reuter, S., A. Buck, O. Grebe, K. Nussle-Kugele, P. Kern, and B. J. Manfras.** 2003. Salvage treatment with amphotericin B in progressive human alveolar echinococcosis. Antimicrob. Agents Chemother. **47:**3586–3591.
14. **Sako, Y., M. Nakao, K. Nakaya, H. Yamasaki, B. Gottstein, M. W. Lightowlers, P. M. Schantz, and A. Ito.** 2002. Alveolar echinococcosis: characterization of diagnostic antigen Em18 and serological evaluation of recombinant Em18. J. Clin. Microbiol. **40:**2760–2765.
15. **Schantz, P. M., J. F. Wilson, S. P. Wahlquist, L. P. Boss, and R. L. Rausch.** 1983. Serologic tests for diagnosis and post-treatment evaluation of patients with alveolar hydatid disease (*Echinococcus multilocularis*). Am. J. Trop. Med. Hyg. **32:**1381–1386.
16. **Tappe, D., M. Frosch, Y. Sako, S. Itoh, B. Grüner, S. Reuter, M. Nakao, A. Ito, and P. Kern.** 2009. Close relationship between clinical regression and specific serology in the follow-up of patients with alveolar echinococcosis in different clinical stages. Am. J. Trop. Med. Hyg. **80:**792–797.
17. **von Gunten, S., D. F. Smith, R. D. Cummings, S. Riedel, S. Miescher, A. Schaub, R. G. Hamilton, and B. S. Bochner.** 2009. Intravenous immunoglobulin contains a broad repertoire of anticarbohydrate antibodies that is not restricted to the IgG2 subclass. J. Allergy Clin. Immunol. **123:**1268–1276.
18. **Wen, H., S. Bresson-Hadni, D. A. Vuitton, D. Lenys, B. M. Yang, Z. X. Ding, and P. S. Craig.** 1995. Analysis of immunoglobulin G subclass in the serum antibody responses of alveolar echinococcosis patients after surgical treatment and chemotherapy as an aid to assessing the outcome. Trans. R. Soc. Trop. Med. Hyg. **89:**692–697.
19. **Wen, H., and P. S. Craig.** 1994. Immunoglobulin G subclass responses in human cystic and alveolar echinococcosis. Am. J. Trop. Med. Hyg. **51:**741–748.
20. **Wen, H., P. S. Craig, A. Ito, D. A. Vuitton, S. Bresson-Hadni, J. C. Allan, M. Rogan, E. Paollilo, and M. Shambesh.** 1995. Immunoblot evaluation of IgG and IgG subclass antibody responses for immunodiagnosis of human alveolar echinococcosis. Ann. Trop. Med. Parasitol. **89:**485–495.

Parasitology International 60 (2011) 108–110

Contents lists available at ScienceDirect

Parasitology International

journal homepage: www.elsevier.com/locate/parint

Short communication

A possible nuclear DNA marker to differentiate the two geographic genotypes of *Taenia solium* tapeworms

Marcello Otake Sato [a,b,*], Yasuhito Sako [b], Minoru Nakao [b], Toni Wandra [b,c], Kazuhiro Nakaya [b], Tetsuya Yanagida [b], Akira Ito [b]

[a] Escola de Medicina, Universidade Federal do Tocantins, Palmas-TO 77001-090, Brazil
[b] Department of Parasitology, Asahikawa Medical University, Asahikawa 078-8510, Japan
[c] Directorate General Disease Control and Environmental Health, Ministry of Health, Jakarta 10560, Indonesia

ARTICLE INFO

Article history:
Received 22 July 2010
Received in revised form 22 September 2010
Accepted 15 November 2010
Available online 23 November 2010

Keywords:
Taenia solium
Nuclear DNA marker
Genotyping

ABSTRACT

Cysticercosis caused by infection with embryonated eggs of the pork tapeworm *Taenia solium* is an important cause of neurological disease worldwide. Based on the phylogenetic analysis of mitochondrial DNA, the pathogen has been divided into two geographic clades, corresponding to Afro-American and Asian genotypes. In this study the genotyping of *T. solium* was carried out by using the nuclear DNA sequences of the immunodiagnostic antigen genes *Ag1V1* and *Ag2*. The two geographic genotypes were supported by the *Ag2* sequences, especially showing unique substitutions in each of the genotypes. It seems likely that the *Ag2* may be a novel nuclear DNA marker to distinguish the two geographic genotypes of *T. solium*.

The larval stage of the pork tapeworm *Taenia solium* is responsible for cysticercosis. Humans are accidentally infected with *T. solium* by ingestion of embryonated eggs excreted with feces of symptomatic and asymptomatic carriers harboring the adult tapeworm in the intestinal tract. The hatched embryos migrate throughout the body of humans and swine, invade mostly skeletal muscle and encyst to form larval cysticerci. The larvae can also reach subcutaneous tissue, eyes and the central nervous system, resulting in neurocysticercosis (NCC). Among human tapeworms, *T. solium* is the most important as the pathogen of emergent or re-emergent zoonosis because the NCC causes focal neurological deficits and seizures in endemic countries [1,2]. The diagnosis of cysticercosis has been done by clinical criteria, computed tomography (CT), nuclear magnetic resonance (NMR) imaging and serology [3,4]. Glycoproteins in the cyst fluid of *T. solium* have been widely used as crude antigens for serodiagnosis [5,6]. Recombinant antigens have been used for the diagnosis of cysticercosis. We demonstrated that the chimeric recombinant protein Ag1V1/Ag2 is a superior antigen for immunodiagnosis in humans and animals [7–11]. Each of the *Ag1V1* and *Ag2* is a gene encoding a low molecular weight backbone protein of the cystic glycoproteins. Our previous phylogenetic analysis of mitochondrial DNA (mtDNA) revealed that *T. solium* individuals can be divided into two geographic clades, corresponding to Afro-American and Asian genotypes [12]. During the analysis process of Western blotting, we also noticed that the banding profiles of crude glycoproteins differ among cyst fluids from geographically different origins [13,14]. In the present study, we evaluated the usefulness of *Ag1V1* and *Ag2* as a nuclear DNA marker to characterize the local isolates of *T. solium*.

A total of 7 geographic samples of *T. solium* cysticerci collected from Indonesia (Papua, former Irian Jaya), India, China, Brazil, Tanzania, Cameroon and South Africa in 1996 through 2001 were examined for this study. All the samples were obtained from muscles of domesticated pigs [14] and were preserved in 70% ethanol until DNA extraction. Genomic DNA was extracted from a single cysticercus by using a spin column kit (DNeasy tissue kit, QIAGEN). Each of *Ag1V1* and *Ag2* genes was amplified by polymerase chain reaction (PCR). Two sets of PCR primers were designed from the cDNA sequences of *Ag1V1* and *Ag2*. The primer pair Ag1V1F (5′-CTC GCT CTC ACT GTA TTC GT-3′) and Ag1V1R (5′-TTG ACA AGT TAA GCA GTT TT-3′) allowed us to amplify the genomic sequence of *Ag1V1*. The amplicons of *Ag2* were obtained by using the primer pair Ag2F (5′-CTC GCT CTC AGT GTT TTC GT-3′) and Ag2R (5′-TTG ACA AGT TAA GCA GCT TC-3′). PCR was carried out in a 50 μl reaction mixture containing 1 μl of template DNA (approximately 100 ng), each dNTP at 200 μM each primer, 1U of DNA polymerase (PrimeSTAR, TaKaRa Biomedicals) and the manufacturer-supplied reaction buffer. For PCR amplification, we employed 30 thermal cycles (94 °C for 30 s, 50 °C for 5 s and 72 °C for 30 s) for both genes. Prior to DNA sequencing, each amplified product was purified by using a PCR clean-up kit (NucleoSpin, Macherey-Nagel). The Bigdye terminator cycle sequencing kit and the ABI PRISM 377 genetic analyzer (Applied Biosystems) were used as recommended by the manufacturer. DNAs were directly sequenced by using PCR primers. In

* Corresponding author. Escola de Medicina, Universidade Federal do Tocantins, Av: NS 15 ALC NO 14, 109 Norte Campus Universitário de Palmas, Palmas, TO CEP77001-090, Brazil. Tel.: +55 63 32328273; fax: +55 63 32328158.
E-mail address: otake@uft.edu.br (M.O. Sato).

1383-5769/$ – see front matter © 2010 Elsevier Ireland Ltd. All rights reserved.
doi:10.1016/j.parint.2010.11.004

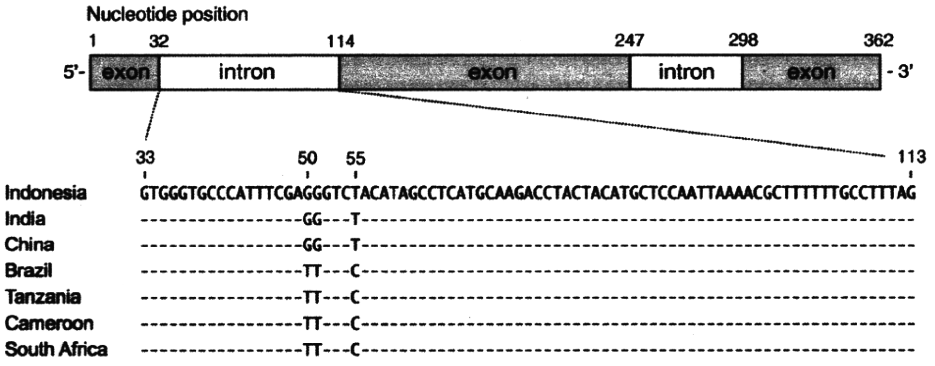

Fig. 1. The exon–intron structure of genomic PCR products for *Ag2* and their multiple alignment showing nucleotide substitutions. The Asian isolates of *T. solium* are originated from Indonesia, India and China, and the Afro-American isolates from Brazil, Tanzania, Cameroon and South Africa.

the case of low amounts of PCR products, the amplicons were subcloned into pGEM-T plasmid vector (Promega) by using an adenine tailing kit (Qiagen). Insert DNAs in the plasmid were read by T7 promoter primer (5′-ATT ATG CTG AGT GAT ATC CC-3′).

As demonstrated by Sato et al. [14], the diagnostic antigen genes *Ag1V1* and *Ag2* are universally present in *T. solium* isolates from Asia, Africa and America. In this study we could amplify the 379 bp fragments of *Ag1V1* and the 362 bp fragments of *Ag2* from all of the isolates examined. After sequencing, we found 3 haplotypes in *Ag1V1* and 2 haplotypes in *Ag2*. Both of the genomic sequences included 2 introns. The nucleotide sequences of *Ag1V1* (DDBJ/EMBL/GenBank accession nos. AB263426–AB263432) contained 2 substitution sites in the second exon and 1 substitution site in the first intron. All of them were transitional changes from thymine to cytosine bases. The two point mutations, which were observed at position 183 in the Brazilian isolate and at position 223 in the Chinese isolate, caused amino acid changes. Although these mutations had no geographic characteristics, more studies on the genetic polymorphisms of *T. solium* in Brazil and China are necessary to determine whether *Ag1V1* is usable as a genetic marker at local level.

As contrasted with *Ag1V1*, the sequences of *Ag2* (AB263419–AB263425) were geographically informative in classifying the isolates. The exon sequences were completely identical among the isolates examined. However, there were 3 substitutions in the first intron. As shown in Fig. 1, transversional substitutions (G and T) occurred at positions 50 and 51, and a transitional substitution (T and C) further occurred at position 55. All of the point mutations were highly correlated with the Afro-American and Asian genotypes of *T. solium*, which were defined from the sequences of mtDNA [12].

The observation of parasitic material is the most important step for diagnosis in parasitology. However, morphological identification is usually difficult in the case that specimens are just a piece of the entire material [15]. The development of DNA markers for *T. solium* worldwide allows us to design a useful tool for diagnosis even if all the morphological characteristics are lost. Based on the sequences of mtDNA, PCR-based techniques such as base excision sequence scanning thymine-base reader analysis, multiplex PCR and DNA sequencing have been used for the molecular identification of adult tapeworms and metacestodes, particularly in differentiating the Afro-American and Asian genotypes of *T. solium* [10,14–16]. However, nuclear DNA markers are still required for the phylogeographic studies of *T. solium* because the maternally inherited haploid mtDNA is unsuitable to use as an ideal marker for population genetics. As shown in this study, the nuclear *Ag2* gene may serve as an alternative DNA marker to determine the geographic genotypes of *T. solium* specimens.

The identification of the genotypes is an important issue on travel medicine programs. In some cases the endemic areas of *T. solium* have natural resources that attract outer people who can become worm carriers for non-endemic areas [9]. Tracking geographic areas where taeniasis/cysticercosis patients became infected may be achieved by examining the genetic polymorphism of *T. solium* [17]. Recently, the coexistence of the Afro-American and Asian genotypes has been found in Madagascar [18]. The nuclear DNA marker of *Ag2* may be useful to detect cross-hybridization events between the two genotypes.

In conclusion, we found a possible nuclear DNA marker to differentiate the geographic genotypes of *T. solium*. More nuclear markers are needed to examine the population genetic structures of *T. solium* worldwide. A panel of the genetic markers will depict the evolutionary tracks of the parasite and humans.

Acknowledgements

This study was supported in part by Grant-in-Aid for Scientific Research from the Japan Society for Promotion of Science (JSPS) (21256003), by the Asia-Africa Scientific Platform Fund (2006–2011), by the Special Cooperation Fund for Promoting Science & Technology, Ministry of Education, Japan (2010–2012) to A. Ito and the National Council for Scientific and Technological Development (CNPq) (502001/2009-7) to M.O. Sato.

References

[1] Schantz PM, Wilkins PP, Tsang VCW. Immigrants, imaging and immunoblots: the emergence of neurocysticercosis as a significant public health problem. In: Scheld WM, Craig WA, Hughes JM, editors. Emerging Infections, 2. Washington, DC: ASM Press; 1998. p. 213–42.
[2] Ito A, Yamasaki H, Nakao M, Sako Y, Okamoto M, Sato MO, et al. Multiple genotypes of *Taenia solium*—ramifications for diagnosis, treatment and control. Acta Trop 2003;87:95–101.
[3] Takayanagui OM, Odashima NS. Clinical aspects of neurocysticercosis. Parasitol Int 2006;55:S111–5.
[4] Ito A, Takayanagui OM, Sako Y, Sato MO, Odashima NS, Yamasaki H, et al. Neurocysticercosis: clinical manifestation, neuroimaging, serology and molecular confirmation of histopathologic specimens. Southeast Asian J Trop Med Public Health 2006;37(Suppl 3):74–81.
[5] Tsang VC, Brand JA, Boyer AE. An enzyme-linked immunoelectrotransfer blot assay and glycoprotein antigens for diagnosing human cysticercosis (*Taenia solium*). J Infect Dis 1989;159:50–9.
[6] Ito A, Plancarte A, Ma L, Kong Y, Flisser A, Cho SY, et al. Novel antigens for neurocysticercosis: simple method for preparation and evaluation for serodiagnosis. Am J Trop Med Hyg 1998;59:291–4.
[7] Sako Y, Nakao M, Ikejima T, Piao XZ, Nakaya K, Ito A. Molecular characterization and diagnostic value of *Taenia solium* low-molecular-weight antigen genes. J Clin Microbiol 2000;38:4439–44.
[8] Ito A, Putra MI, Subahar R, Sato MO, Okamoto M, Sako Y, et al. Dogs as alternative intermediate hosts of *Taenia solium* in Papua (Irian Jaya), Indonesia confirmed by highly specific ELISA and immunoblot using native and recombinant antigens and mitochondrial DNA analysis. J Helminthol 2002;76:311–4.
[9] Sato MO, Yamasaki H, Sako Y, Nakao M, Nakaya K, Plancarte A, et al. Evaluation of tongue inspection and serology for diagnosis of *Taenia solium* cysticercosis in swine: usefulness of ELISA using purified glycoproteins and recombinant antigen. Vet Parasitol 2003;111:309–22.

[10] Sato MO, Cavalcante TV, Sako Y, Nakao M, Yamasaki H, Yatsuda AP, et al. Evidence and potential for transmission of human and swine *Taenia solium* cysticercosis in the Piracuruca region, Piauí, Brazil. Am J Trop Med Hyg 2006;75:933–5.
[11] Sako Y, Nakao M, Nakaya K, Yamasaki H, Ito A. Recombinant antigens for serodiagnosis of cysticercosis and echinococcosis. Parasitol Int 2006;55(Suppl): S69–73.
[12] Nakao M, Okamoto M, Sako Y, Yamasaki H, Nakaya K, Ito A. A phylogenetic hypothesis for the distribution of two genotypes of the pig tapeworm *Taenia solium* worldwide. Parasitology 2002;124:657–62.
[13] Ito A, Nakao M, Okamoto M, Sako Y, Yamasaki H. Mitochondrial DNA of *Taenia solium* cysticercosis: from basic to applied science. In: Singh G, Prabhakar S, editors. *Taenia solium* from Basic to Clinical Science. Wallingford, UK: CABI Publishing; 2002. p. 47–55.
[14] Sato MO, Sako Y, Nakao M, Yamasaki H, Nakaya K, Ito A. Evaluation of purified *Taenia solium* glycoproteins and recombinant antigens in the serologic detection of human and swine cysticercosis. J Infect Dis 2006;194:1783–90.
[15] Yamasaki H, Allan JC, Sato MO, Nakao M, Sako Y, Nakaya K, et al. DNA differential diagnosis of taeniasis and cysticercosis by multiplex PCR. J Clin Microbiol 2004;42: 548–53.
[16] Yamasaki H, Nakao M, Sako Y, Nakaya K, Sato MO, Mamuti W, et al. DNA differential diagnosis of human taeniid cestodes by base excision sequence scanning thymine-base reader analysis with mitochondrial genes. J Clin Microbiol 2002;40:3818–21.
[17] Yanagida T, Yuzawa I, Joshi DD, Sako Y, Nakao M, Nakaya K, et al. Neurocysticercosis: assessing where the infection was acquired from. J Travel Med 2010;17: 206–8.
[18] Michelet L, Carod JF, Rakontondrazaka M, Ma L, Gay F, Dauga C. The pig tapeworm *Taenia solium*, the cause of cysticercosis: biogeographic (temporal and spacial) origins in Madagascar. Mol Phylogenet Evol 2010;55:744–50.

Experimental Parasitology xxx (2010) xxx–xxx

Contents lists available at ScienceDirect

Experimental Parasitology

journal homepage: www.elsevier.com/locate/yexpr

Echinococcus multilocularis: Identification and functional characterization of cathepsin B-like peptidases from metacestode ☆

Yasuhito Sako [a,*], Kazuhiro Nakaya [b], Akira Ito [a]

[a] Department of Parasitology, Asahikawa Medical University, Midorigaoka Higashi 2-1, Asahikawa, 078-8510 Hokkaido, Japan
[b] Animal Laboratory for Medical Research, Asahikawa Medical University, Midorigaoka Higashi 2-1, Asahikawa, 078-8510 Hokkaido, Japan

ARTICLE INFO

Article history:
Received 14 September 2010
Received in revised form 12 November 2010
Accepted 16 November 2010
Available online xxxx

Keywords:
Cestode
Echinococcus multilocularis
Metacestode
Cathepsin B-like peptidase
Recombinant enzyme
Host proteins

ABSTRACT

Cysteine peptidases have potent activities in the pathogenesis of various parasitic infections, and are considered as targets for chemotherapy and antigens for vaccine. In this study, two cathepsin B-like cysteine peptidases (EmCBP1 and EmCBP2) from *Echinococcus multilocularis* metacestodes were identified and characterized. Immunoblot analyses demonstrated that EmCBP1 and EmCBP2 were present in excretory/secretory products and extracts of *E. multilocularis* metacestodes. By immunohistochemistry, EmCBP1 and EmCBP2 were shown to localize to the germinal layer, the brood capsule and the protoscolex. Recombinant EmCBP1 and EmCBP2 expressed in *Pichia pastoris*, at optimum pH 5.5, exhibited substrate preferences for Z-Phe-Arg-MCA, Z-Val-Val-Arg-MCA, and Z-Leu-Arg-MCA, and low levels of hydrolysis of Z-Arg-Arg-MCA. Furthermore, recombinant enzymes degraded IgG, albumin, type I and IV collagens, and fibronectin. These results suggested that EmCBP1 and EmCBP2 may play key roles in protein digestion for parasites' nutrition and in parasite–host interactions.

1. Introduction

Alveolar echinococcosis (AE), caused by the larval stage of *Echinococcus multilocularis*, is a serious parasitic disease of humans in countries of the higher latitudes of Northern Hemisphere. In the previous decade, a lot of new data have been published on prevalence of *E. multilocularis* in final and intermediate hosts in areas where it had previously not been recorded (Eckert et al., 2000; Ito et al., 2010). Humans are accidentally infected with *E. multilocularis* by ingestion of eggs excreted with the feces of carnivores harboring adult tapeworm of this species. It is thought that humans become exposed to *E. multilocularis* by handling of infected definitive hosts, or by ingestion of food and water contaminated with eggs. Oncospheres hatched from eggs in the small intestine of humans migrate via the portal system into various organs, mainly liver and differentiate and develop into the metacestode stage. The metacestodes propagate asexually like a tumor leading to organ dysfunction. Since clinical symptoms usually do not become evident until 10 or more years after initial parasite infection, early diagnosis and treatment especially during asymptomatic period are important for reduction of morbidity and mortality (McManus et al., 2003). About one third of patients have cholestatic jaundice and about one third of patients have epigastric pain. In the remaining patients, *E. multilocularis* infections are incidentally detected during medical examination for symptoms such as fatigue, weight loss, hepatomegaly (Pawlowski et al., 2001). In addition to surgical removal of alveolar hydatid cyst, treatment with antiparasitic agents, benzimidazole derivatives, is the most important for AE therapy. However, these drugs have parasitostatic activity rather than parasitocidal activity, and side-effects such as liver damage are often observed with long-term administration (Kern, 2006). Thus, it is urgent to develop novel reliable chemotherapeutic agents.

Cysteine peptidases belonging to clan CA family C1 (Rawlings et al., 2004; http://merops.sanger.ac.uk/) besides their housekeeping functions such as protein turnover in parasite cells are involved in evasion from host immune responses, essential nutrient uptake, and tissue penetration, by degrading host proteins, including immunoglobulin, complement components, kininogen, haemoglobin, albumin, and extracellular matrix proteins (reviewed by Sajid and McKerrow 2002; Dalton et al., 2003; Caffrey et al., 2004; Rosenthal, 2004; McKerrow et al., 2006; Robinson et al., 2008; Smooker et al., 2010). Furthermore, some cysteine peptidases have activities to stimulate human eosinophils to induce degranulation (Shin et al., 2005), deplete CD4 positive human lymphocytes *in vitro* (Molinari et al., 2000), induce apoptosis in human CD4 positive cells (Tato et al., 2004), by interacting with host cells via unknown mechanisms. Therefore, cysteine peptidases of parasites are considered as important targets for chemotherapy and/or

☆ *Note*: The nucleotide sequence data reported in this study are available in the GenBank, EMBL, and DDBJ databases under accession numbers AB586072 (EmCBP1) and AB586073 (EmCBP2).

* Corresponding author. Fax: +81 166 68 2429.
E-mail address: yasusako@asahikawa-med.ac.jp (Y. Sako).

0014-4894/$ - see front matter © 2010 Elsevier Inc. All rights reserved.
doi:10.1016/j.exppara.2010.11.005

immunoprophylaxis (Dalton et al., 2003; Barr et al., 2005; Abdulla et al., 2007; Alcala-Canto et al., 2007).

E. multilocularis metacestodes survive for many years in human host, which leads us to consider peptidases as important parasite components to evade from host immune responses and to uptake nutrient. However, precise characterization of *E. multilocularis* peptidases essential to develop enzyme inhibitors has been hampered by the difficulty of obtaining pure parasite materials, since parasite materials obtained from laboratory animals are contaminated with numerous host cells resulting from that *E. multilocularis* infiltrate and proliferate by exogenous budding of the germinative cells in host tissue (Thompson, 1995). Recently, we have succeeded in cloning of cathepsin L-like peptidase genes (EmCLP1 and EmCLP2) from *E. multilocularis* metacestodes, which enabled us to prepare a large amount of parasite enzymes for detailed characterizations (Sako et al., 2007). Activities of recombinant EmCLP1 and EmCLP2 to degrade human IgG, bovine albumin, type I and type IV collagen and fibronectin have been demonstrated, which suggests their important roles in parasite growth and survival in the host. In the present study, we have identified two genes encoding cathepsin B-like cysteine peptidases from *E. multilocularis* metacestodes. Immunoblot analyses with monoclonal antibody detected both enzymes in crude metacestode extract and ES products, and immunohistochemical studies revealed that both enzymes are expressed in the germinal layer, the brood capsule, and the protoscolex. Moreover, enzymatic activities against synthetic peptide substrates and macromolecule proteins were also characterized by using recombinant active enzymes expressed in *Pichia pastoris*.

2. Materials and methods

2.1. Animals

Animal procedures and management protocols in this study were approved by the Ethics Committee of Asahikawa Medical University, Asahikawa, Japan.

2.2. Preparation of parasite material

E. multilocularis (Furano isolate, Hokkaido, Japan) metacestode tissue was obtained from non-obese diabetic severe combined immunodeficiency (NOD/Shi-*scid*) mice infected by intraperitoneal passage of metacestodes (Nakaya et al., 2006). Microvesicle and protoscolex suspensions were prepared by pressing metacestode tissue through a 300 μm metal mesh with PBS. The microvesicles and protoscoleces were washed five to seven times with PBS, and then used for preparation of metacestode crude lysate and excretory/secretory (ES) products. Because NOD/Shi-*scid* mice had little inflammatory response, isolation of microvesicles and protoscoleces with less host components, which are commonly found in those from immunocompetent mice, could be done efficiently.

To prepare metacestode crude lysate, microvesicles and protoscoleces were homogenized with three times volume of lysis buffer consisting of 20 mM Tris–HCl, pH 7.4, 150 mM NaCl, and 1.0% 3-[(3-cholamidopropyl)dimethylammonia]-1-propanesulfonic acid (CHAPS) in the presence of peptidase inhibitors (protease inhibitor cocktail for mammalian tissues, Sigma–Aldrich). After one freeze–thaw cycle and centrifugation at 10,000*g* for 30 min at 4 °C, the supernatant was recovered and kept at −80 °C until use.

To obtain ES products, microvesicles and protoscoleces were cultured in RPMI-1640 medium supplemented with 100 U/ml penicillin and 100 μg/ml streptomycin at 37 °C for 12 h. Few dead microvesicles and protoscoleces were found under a microscopic examination at the end of cultivation, which indicated that the contamination of intracellular proteins released into the medium supernatant as a result of parasite death had been almost completely avoided. The medium supernatant containing ES products was carefully collected and was passed through a disposable chromatography column (Econo-Pac column, Bio-Rad) with a porous bed support (a 30 μm pore size) to remove minor microvesicle and protoscolex contaminants. After filtration through 0.45 μm filter membrane (Millipore), the medium supernatant was concentrated by using an Amicon Ultra-15 Centrifugal Filter Unit with a cutoff size of 5 kDa (Millipore) and kept at −80 °C until use.

2.3. Cloning of EmCBP1 and EmCBP2 genes

Total RNA was isolated from freshly prepared *E. multilocularis* metacestodes using Trizol reagent (Gibco BRL) according to the manufacture's instruction. After purification of Poly(A)$^+$ RNA by using oligo(dT)-latex beads (TaKaRa), cDNA available in 5′ and 3′ rapid amplification of cDNA end (RACE) method was synthesized from 1 μg of purified poly(A) $^+$ RNA by using the GeneRacer Kit (Invitrogen).

3′ RACE were performed with degenerated forward primers designed from the consensus sequences flanking the active site residues of eukaryotic cysteine peptidases and 3′ RACE primer.

The forward primer (5′-CAGGGTCAGTGYGGNTCNTGYTGG-3′) and GeneRacer 3′ primer (5′-GCTGTCAACGATACGCTACGTAACG-3′) were used in the first round PCR, and the forward primer (5′-CAGTGCGGTTCNTGYTGGGCNTTY-3′) and GeneRacer 3′ Nested primer (5′-CGCTACGTAACGGCATGACAGTG-3′) were used in the nested PCR. PCR reactions were performed in a 50 μl of reaction mixture containing 1 × *Ex Taq* Buffer, 2.0 mM $MgCl_2$, 0.2 μM of each primer, 0.2 mM of each dNTP, 5 ng of cDNA and 0.5 units of *EX Taq* DNA polymerase (TaKaRa) and cycling conditions were 30 s at 94 °C (first cycle: 2 min at 94 °C), 30 s at 50 °C and 30 s at 72 °C for 30 cycles. The PCR products were separated in a 1.0% agarose gel, the DNA fragments were recovered and cloned into pGEM T-vector (Promega), and plasmid clones were sequenced. To obtain sequence upstream of EmCBP1 and EmCBP2 genes, 5′ RACE was performed using gene-specific primer (5′-CGTACCATCACTGCTC TCCCGCTTACTGTC-3′ for EmCBP1gene, 5′-TGCAACCAAAGCCACAG AATAAGCC-3′ for EmCBP2 gene) and GeneRacer 5′ primer (5′-CG ACTGGAGCACGAGGACACTGA-3′) with annealing temperature of 60 °C. Finally, full-length cDNAs of the EmCBP1 and EmCBP2 genes were cloned by PCR using a high-fidelity DNA polymerase, Phusion DNA polymerase (Finnzymes), and primers directed to both the UTR ends.

2.4. Expression of the mature region of EmCBP1 and EmCBP2 in Escherichia coli and purification

The mature enzyme region of EmCBP1 or EmCBP2 was amplified by PCR with primer sets containing a restriction enzyme (underlined) recognition sequence added to 5′ end to facilitate cloning of the PCR products. The primers used were: 5′-GGGAATTC CTGCCGGCATCTTTTGATCCC-3′ (mCBP1/F), 5′-GGGTCGACTAGTT TTGTGGGATACCTGC-3′ (CBP1/R), 5′-GGGAATTCCTTCCCTCAGAAT TTGACGCA-3′ (mCBP2/F), 5′-GGGTCGACTCACTTCCTTATTTTTGGA ATACC-3′ (CBP2/R). The PCR reactions were performed with cDNA clones as templates. The PCR products were digested with *Eco*RI and *Sal*I, cloned into bacterial expression vector pET-30a(+) (Novagen) for producing a fusion protein with His tag. The cloned plasmids were transfected into *E. coli* BL21(DE3)pLysS strain. Expression of recombinant proteins was induced by addition of 1 mM isopropyl-β-D-thiogalactoside (IPTG) to the culture. Recombinant proteins were purified using Ni-NTA beads (Qiagen) under denaturation conditions. Protein concentration was determined by BCA protein assay kit (Pierce).

Please cite this article in press as: Sako, Y., et al. *Echinococcus multilocularis*: Identification and functional characterization of cathepsin B-like peptidases from metacestode. Exp. Parasitol. (2010), doi:10.1016/j.exppara.2010.11.005

2.5. Production of monoclonal antibodies

Female BALB/c mice were immunized by intraperitoneally (i.p.) injection of 50 μg of *E. coli*-expressed recombinant EmCBP1 (eEmCBP1) or EmCBP2 (eEmCBP2) emulsified in Freund's complete adjuvant. Three weeks later the procedure was repeated but with Freund's incomplete adjuvant. Three days before the fusion, the mice were i.p. boosted with 50 μg antigens in PBS. Spleen cells of mice were fused with NS-1 myeloma cells. The antibody-secreting hybridomas were screened by ELISA with eEmCBP1 or eEmCBP2. Hybridomas selected were cloned by limit dilution at least twice.

2.6. SDS–PAGE and immunoblot analysis

Proteins were treated with a SDS sample buffer (62.5 mM Tris–HCl, pH 6.8, 2.0% SDS, 50 mM dithiothreitol and 10.0% glycerol) at 100 °C for 5 min and separated in a 7.5% or 12.5% polyacrylamide gel. For immunoblot analysis, the separated proteins were transferred onto a polyvinylidene difluoride (PVDF) membrane sheet (Millipore). The sheet was blocked with blocking solution (20 mM Tris–HCl, pH 7.6, 150 mM NaCl, 1.0% casein, 0.1% Tween 20) and probed with monoclonal antibody followed by alkaline phosphatase-conjugated anti-mouse IgG antibody (Novagen). Nitroblue tetrazolium/5-bromo-4-chloro-3-indoyl phosphate was used for color development.

2.7. Immunohistochemistry

Parasite tissues and livers from infected-NOD/Shi-*scid* mice were washed once with PBS and fixed with 2.0% paraformaldehyde in PBS overnight at 4 °C and then embedded in paraffin. Sections of 5 μm were produced and were transferred to slides. After antigen retrieval using HistoVT One (Nacalai Tesque), sections were treated with peroxidase blocking solution (0.3% H_2O_2 in methanol) for 30 min. Then, sections were washed with PBS, blocked using blocking solution for 1 h and incubated overnight at 4 °C with monoclonal antibody. After three washing with PBS, the sections were incubated with peroxidase-conjugated anti-mouse IgG antibody (ImmPRESS REAGENT, Vector laboratories) for 30 min at room temperature. After four washing with PBS, the sections were incubated with 3-amino-9-ethylcarbazole. All sections were counterstained with hematoxylin.

2.8. Expression of EmCBP1 and EmCBP2 in P. pastoris

The pro-mature coding region of EmCBP1 or EmCBP2 was amplified by PCR with primer sets containing a restriction enzyme (underlined) recognition sequence. The primers used were: 5′-CGGAATTCA GTACTGTGACCAGCGCAATTGG-3′ (proCLP1/F), 5′-ATGCGGCCGCTA GTTTTGTGGGATACCTGC-3′ (PIC CLP1/R), 5′-CGGAATTCAGAAAACC TCATCAGAGCGAC-3′ (proCLP2/F), 5′-ATGCGGCCGCTCACTTCCTTA TTTTTGGAATACC-3′ (PIC CBP2/R). The PCR reactions were carried out as mentioned above. The PCR products were digested with *Eco*RI and *Not*I and cloned into yeast expression vector pPICZα A (Invitrogen), and subsequently linearized with *Pme*I and electroporated into *P. pastoris* KM71 host cells. Yeast transformants were cultured in 500 ml of buffered-glycerol complex medium (1.0% yeast extract, 2.0% peptone, 1.34% yeast nitrogen base, 4×10^{-5}% biotin, 1.0% glycerol, and 100 mM potassium phosphate, pH 6.0) at 28 °C for 2 days and collected by centrifugation at 1000*g* for 5 min, and protein expressions were induced by resuspending the cells in 100 ml of buffered-methanol minimal medium (1.34% yeast nitrogen base, 4×10^{-5}% biotin, 1.0% methanol, and 100 mM potassium phosphate, pH 6.0) at 28 °C for 3 days. Due to the presence of an α-factor leader peptide sequence, recombinant proteins were secreted into expression medium. The culture medium containing recombinant EmCBP1 (yEmCBP1) or EmCBP2 (yEmCBP2) was collected, concentrated using an Amicon stirred cell with a YM-10 membrane and dialyzed against 50 mM sodium acetate buffer (pH 4.5) containing 2.5 mM EDTA. For purification of active form of yEmCBP1, dialysate was directly loaded on a HisTrap SP XL cation-exchange column pre-equilibrated with 50 mM sodium acetate buffer (pH 4.5) containing 2.5 mM EDTA after activation at 37 °C for 1 h in the presence of 10 mM L-cysteine and proteins were eluted by use of a linear salt gradient (0–1.0 M NaCl). For purification of active form of yEmCBP2, the conversion of pro-form into active enzyme was accomplished by treatment with pepsin. After addition of porcine pepsin (Sigma–Aldrich) at a final concentration of 0.5 mg/ml, the activation mixture was incubated at 37 °C for 4 h. The activated yEmCBP2 was purified as mentioned above. Recombinant proteins were treated with peptide:*N*-glycosidase F (PNGase F, New England Biolabs) under denaturing conditions to remove any N-linked oligosaccharides to determine whether recombinant proteins were glycosylated.

2.9. Irreversible active site-labelling of yEmCBP1 and yEmCBP2

A biotinylated dipeptidyl fluoromethylketone (Biotin-Phe-Ala-FMK, MP Biomedicals), a cysteine peptidase inhibitor, was used for active-site labelling. Briefly, the purified enzyme was incubated for 30 min at room temperature with 10 μM biotin-Phe-Ala-FMK in 100 mM sodium acetate buffer (pH 5.5) containing 2.5 mM EDTA, 0.1% CHAPS and 10 mM L-cystine. Labelled proteins were detected with alkaline phosphatase-conjugated streptavidin (Novagen).

2.10. Substrate specificity and kinetic measurements of yEmCBP1 and yEmCBP2

Peptidase activity was characterized by using peptidyl-4-methylcoumarin-7-amide (MCA) as substrates. The standard assay volume was 200 μl, using 100 mM sodium acetate buffer (pH 5.5) containing 0.1% CHAPS, 2.5 mM EDTA and 10 mM L-cysteine. Substrates were added to a final concentration of 2 μM, or other concentration as required. Assays were performed at room temperature. The amount of 7-amino-4-methylcoumarin (AMC) released was measured by the fluorometer (VersaFluor Fluorometer, Bio-Rad) at an excitation wavelength of 370 nm and an emission wavelength of 460 nm.

For determination of the optimum pH of recombinant enzyme activity, 100 mM citrate–phosphate buffer (pH 3.0–8.0) containing 250 mM NaCl, 0.1% CHAPS, 2.5 mM EDTA and 10 mM L-cystine, were used. Substrate specificities were investigated using benzyloxycarbonyl (Z)-Phe-Arg-MCA, Z-Arg-Arg-MCA, Z-Leu-Arg-MCA, Z-Gly-Pro-Arg-MCA, and Z-Val-Val-Arg-MCA at a concentration of 2 μM. The values of K_m and V_{max} for Z-Phe-Arg-MCA and Z-Arg-Arg-MCA were determined by a nonlinear regression analysis. The molar concentration of active recombinant enzymes was determined by active-site titration using the Z-Phe-Arg-MCA and cysteine peptidase inhibitor *trans*-epoxysuccinyl-L-leucylamido(4-guanidino)butane (E-64) as described by Barrett and Kirschke (1981). All peptidyl-MCA substrates used were purchased from Peptide Institute, Japan.

2.11. Inactivation kinetics of yEmCTB1 and yEmCTB2

Inactivation of recombinant enzyme was performed in 100 mM citrate–phosphate buffer (pH 6.5, 7.0, and 7.5) containing 250 mM NaCl, 0.1% CHAPS, 2.5 mM EDTA, and 10 mM L-cystine in the presence of 50 μM Z-Phe-Arg-MCA. Progress of the reaction was monitored continuously by the fluorescence of the released products for 30 min. All progress curves obtained were exponential, and could be best fitted to the following first-order relationship (Eq. 1):

Please cite this article in press as: Sako, Y., et al. *Echinococcus multilocularis*: Identification and functional characterization of cathepsin B-like peptidases from metacestode. Exp. Parasitol. (2010), doi:10.1016/j.exppara.2010.11.005

$$P = P_{\infty}(1 - e^{k_{obs}t})$$

where P and P_{∞} are the product concentration at a given or infinite time, respectively, and k_{obs} is the observed first-order inactivation rate constant. And half-lives were calculated as $t_{1/2} = \ln 2/k_{obs}$.

2.12. Protein substrate digestion

Human IgG, human serum albumin (HSA), soluble calf skin type I collagen, human placenta type IV collagen, and bovine plasma fibronectin were used as protein substrates. All protein substrates used were purchased from Sigma–Aldrich, Japan. Active recombinant enzyme (0.2 μM) was incubated with 0.2 mg/ml of each protein substrate in 100 mM sodium acetate buffer (pH 5.5) containing 2.5 mM EDTA and 10 mM L-cysteine at 37 °C for 4 h. The digestion reaction was stopped by the adding of SDS–PAGE sample buffer. Protein substrate digests were subjected to SDS–PAGE and degradation products were visualized by Coomassie Blue staining.

3. Results

3.1. Primary structure of EmCBP1 and EmCBP2

Following PCR with degenerate primers and sequencing analysis of 48 PCR product clones, a total of four different partial genes encoding cysteine peptidases were obtained from *E. multilocularis* metacestode cDNA. Database search of the deduced amino acid sequences of individual clones revealed that two clones are identical to EmCLP1 and EmCL2 (Sako et al., 2007), respectively, and other two clones show high homology to cathepsin B-like peptidases. Rapid amplification of cDNA ends (RACE) was performed to obtain the full-length of two novel cysteine peptidase cDNAs, termed EmCBP1 and EmCBP2, respectively.

As shown in Fig. 1, EmCBP1 consists of a 18-residue putative signal sequence predicted by the method of Nielsen et al. (1997), a 77-residue propeptide and the 256-residue mature enzyme. EmCBP2 consists of a 16-residue putative signal sequence, a 67-residue propeptide and the 255-residue mature enzyme. Comparison of EmCBP1 with EmCBP2 revealed an amino acid identity of 60.5% (65.6% for the mature region only). The catalytic triad residues are conserved with other crucial residues shaping an oxyanion hole (Menard et al., 1991), and the occluding loop region (Musil et al., 1991) responsible for peptidyldipeptidase activity, a unique feature of cathepsin B, is also present in the mature enzyme. The predicted molecular masses of the mature EmCBP1 and EmCBP2 are 28,241 and 28,140 Da, respectively. In mature region, EmCBP1 has one putative N-linked glycosylation site at position 116.

3.2. Detection of EmCBP1 and EmCBP2 in E. multilocularis

Immunoblot analyses of *E. multilocularis* metacestode crude lysate (Fig. 2, lanes 1) and ES products (lanes 2) were performed. Anti-EmCBP1 monoclonal antibody recognized proteins of 24.5

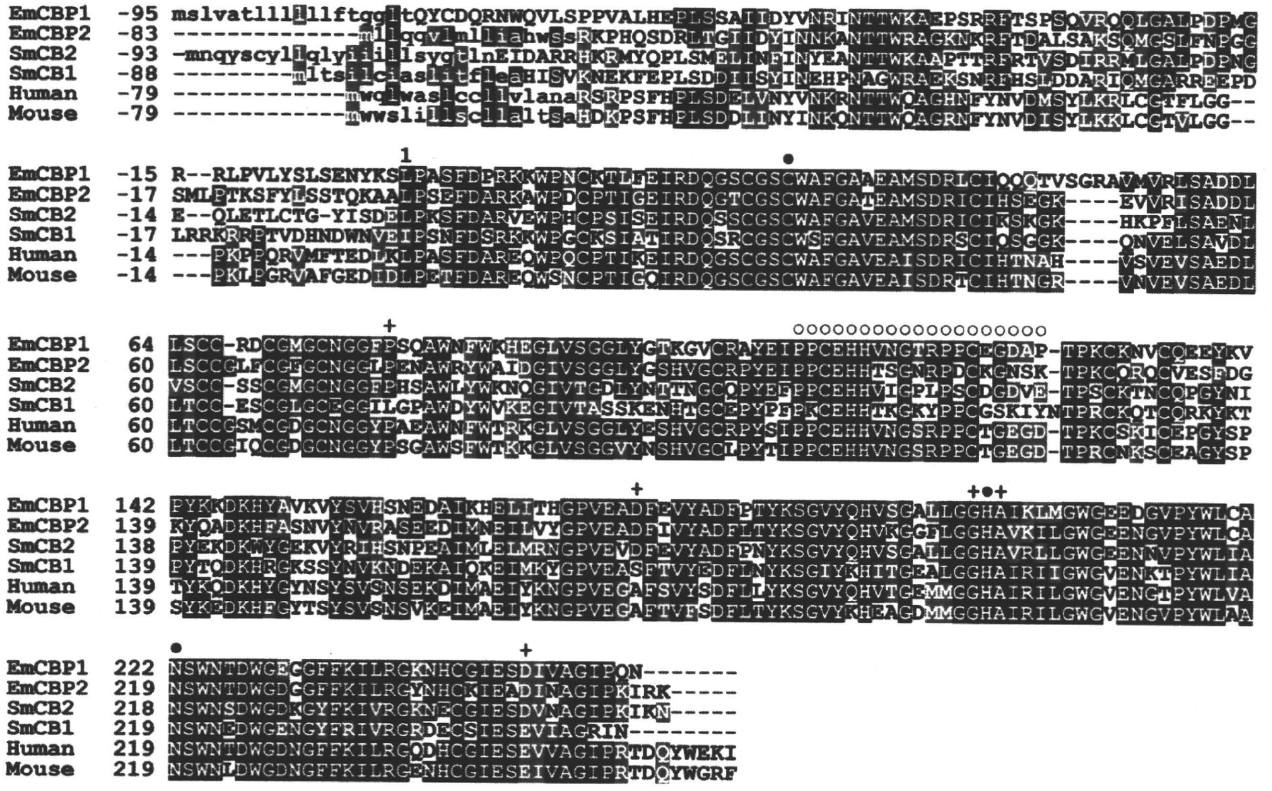

Fig. 1. Comparison of the deduced amino acid sequences of EmCBP1 and EmCBP2 with other cathepsin B enzymes. The alignment was generated using Clustal W server (http://www.ch.embnet.org/software/ClustalW.html) together with BOXSHADE server (http://www.ch.embnet.org/software/BOX_form.html). Gaps were introduced to maximize the alignment. Conserved residues are highlighted: identical, similar and unrelated residues with black, gray, and white backgrounds. Predicted signal sequence is written in lower case and closed circles (●) represent active site residues. Amino acid residues forming substrate binding pockets (McGrath, 1999) are indicated by plus signs (+), and the occluding loop unique to cathepsin B is indicated by open circles (○). Aligned amino acid sequences are *Schistosoma mansoni* cathepsin B (SmCB2, AJ312106), *Schistosoma mansoni* cathepsin B (SmCB1, AAA29865), human cathepsin B (Human, NP_001899), and mouse cathepsin B (Mouse, 1701299A).

Please cite this article in press as: Sako, Y., et al. *Echinococcus multilocularis*: Identification and functional characterization of cathepsin B-like peptidases from metacestode. Exp. Parasitol. (2010), doi:10.1016/j.exppara.2010.11.005

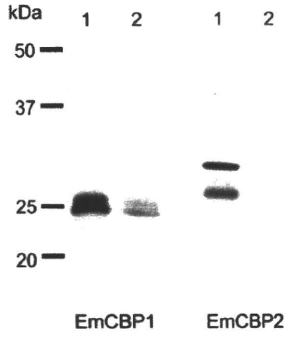

Fig. 2. Immunoblot analyses of *E. multilocularis* metacestodes extracts and ES products. Extracts of *E. multilocularis* metacestodes (lanes 1), and ES products (lanes 2) were probed with anti-EmCBP1 (left) and anti-EmCBP2 (right) monoclonal antibody. Molecular size markers are indicated on the left.

and 25.5 kDa in lysate and ES products, and anti-EmCBP2 monoclonal antibody recognized proteins of 27.0 and 29.9 kDa in lysate and ES products. Isotype-matched negative control monoclonal antibody did not bind to any of these bands (data not shown).

Furthermore, immunohistochemical studies were performed to investigate the localizations of EmCBP1 and EmCBP2 in metacestode. As shown in Fig. 3, the germinal layer, the brood capsule, and the protoscolex were stained. No signals were obtained for the acellular laminated layer of parasite.

3.3. Expression of EmCBP1 and EmCBP2 in yeast

To generate functional peptidases for *in vitro* studies, recombinant EmCBP1(yEmCBP1) and EmCBP2 (yEmCBP2) were expressed in yeast using the *P. pastoris* system and the α-pheromone signal sequence for extracellular secretion. The culture supernatant was collected after 3 days of cultivation and was 20-fold concentrated. The hydrolysis activity of the supernatant treated with and without pepsin in the presence of a reducing agent L-cysteine against Z-Phe-Arg-MCA was tested to determine optimal activation conditions of recombinant enzymes before purification (Fig. 4A). yEmCBP1 was activated at pH 4.5 after 1 h without the pepsin treatment. In contrast, removal of pro-region by pepsin was required for activation of yEmCBP2 (Fig. 4A). The activated recombinant enzyme purified by cation-exchange chromatography as a single peak was analyzed by SDS–PAGE followed by Coomassie Blue staining and immunoblotting (Fig. 4B and C). The purified yEmCBP1 migrated as a broad band between 25 and 50 kDa, and the purified yEmCBP2 migrated as a single band of approximately 27.0 kDa. Treating yEmCBP1 with PNGase F converted the broad band to two bands at 30 and 25.6 kDa (Fig. 4C, lanes 1 and 2), whereas no change in size of yEmCBP2 was observed (Fig. 4C, lanes 3 and 4), which indicated that yEmCBP1 was glycosylated. Analyses using the probe, biotin-Z-Phe-Ala-FMK, able to label specifically active cysteine peptidases revealed that in yEmCBP1 enzymes ranging from 30 to 50 kDa, detected as a 30 kDa band after treated with PNGase F, are active (Fig. 4D, lanes 1 and 2). No active enzyme bands except the 27-kDa enzyme were detected in yEmCBP2 (Fig. 4D, lanes 3 and 4). The labelling of active enzymes with biotin-Phe-Ala-FMK failed by pre-treatment with a cysteine inhibitor, E64 (data not shown).

3.4. Activity of yEmCBP1 and yEmCBP2 against peptidyl-MCA substrates

The substrate specificity of the yEmCBP1 and yEmCBP2 was characterized by using several peptide substrates varying at P2 position (Fig. 5). yEmCBP1 preferred substrates with Phe > Val > Leu at P2 position at an acidic pH optimum of 5.5. Substrate with Pro or Arg at P2 position was also hydrolyzed, but less efficiently. The pH optimum for hydrolyzing substrate with Arg at P2 was shifted to 7.5. yEmCBP2 showed similar features to those of yEmCBP1 except that a marked shifting of the pH optimum for hydrolyzing substrate with Arg at P2 was not observed. yEmCBP2 hydrolyzed peptidyl-MCA substrates more efficiently than yEmCBP1.

Kinetic parameters for hydrolysis of Z-Phe-Arg-MCA (suitable substrate for cathepsin L and B) and Z-Arg-Arg-MCA (cathepsin B-selective substrate) were summarized in Table 1. yEmCBP1 and yEmCBP2 had greater k_{cat}/K_m value for Z-Phe-Arg-MCA over Z-Arg-Arg-MCA. Difference in k_{cat}/K_m values between two substrates for yEmCBP1 and yEmCBP2 was 93- and 137-fold, respectively.

3.5. Inactivation kinetics of yEmCBP1 and yEmCBP2

The kinetics of the pH-induced inactivation of yEmCBP1 and yEmCBP2 were studies at pH 6.5, 7.0, and 7.5, and the reaction between enzymes and substrates (Z-Phe-Arg-MCA) was monitored continuously (Fig. 6 and Table 2). The inactivation of yEmCBP1 at pH 6.5 or 7.0 was not observed during monitoring period and its half-time at pH 7.5 was approximately 318 s. The half-time of yEmCBP2 shortened, from approximately 1689 to 10 s, with increasing pH.

3.6. Degradation of macromolecules by yEmCBP1 and yEmCBP2

To investigate the ability of yEmCBP1 and yEmCBP2 to degrade macromolecules, protein digestion analyses were performed (Fig. 7). In these studies, human IgG and human serum albumin

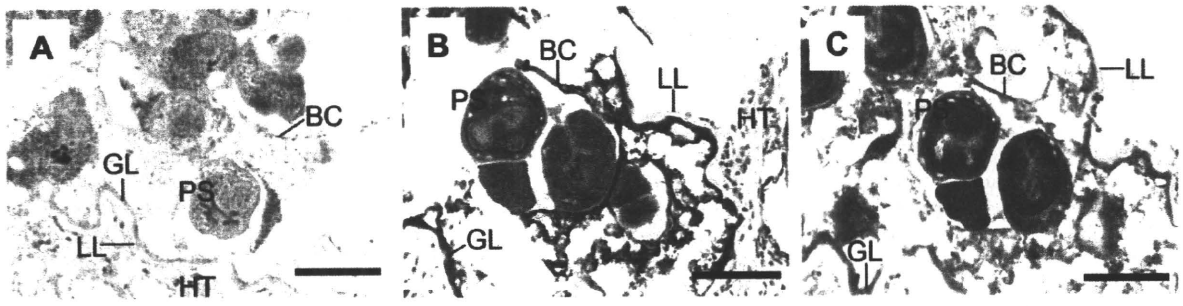

Fig. 3. Immunohistochemical detection of EmCBP1 and EmCBP2 in *E. multilocularis* metacestodes. Parasite tissues (A, B, and C) were isolated and paraffin-sections were produced. The sections were probed with anti-EmCBP1 (B), anti-EmCBP2 (C) and isotype-matched negative control (A) monoclonal antibody. The following structures are indicated: PS, protoscolex; GL, germinal layer; BC, brood capsule; LL, laminated layer; HT, host tissue. Scale bar = 100 μm.

Please cite this article in press as: Sako, Y., et al. *Echinococcus multilocularis*: Identification and functional characterization of cathepsin B-like peptidases from metacestode. Exp. Parasitol. (2010), doi:10.1016/j.exppara.2010.11.005

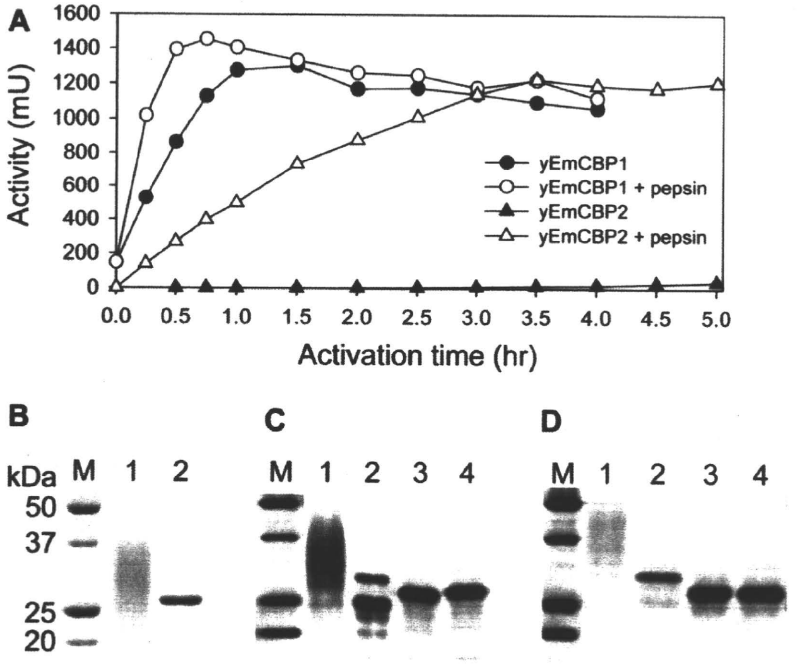

Fig. 4. Expression, purification and active-site labelling of yEmCBP1 and yEmCBP2. (A) Time-dependent activations with and without the pepsin treatment. Aliquots were withdrawn from the incubation mixture at the indicated time points, and the activities were monitored with 50 μM Z-Phe-Arg-MCA. (B) Purified recombinant enzymes were subjected to SDS–PAGE and stained with Coomassie blue. Lane 1, yEmCBP1; lane 2, yEmCBP2. (C) Immunoblot analyses of purified recombinant enzymes before (lanes 1 and 3) and after (lanes 2 and 4) deglycosylation by the treatment with PNGase F. yEmCBP1 (lanes 1 and 2) and yEmCBP2 (lanes 3 and 4) were detected by using monoclonal antibody specific for each protein. (D) Detection of active recombinant enzymes by labelling of purified recombinant proteins with the cysteine peptidase-specific probe, biotin-Phe-Ala-FMK. After labelling, aliquots of recombinant enzymes were treated with (lanes 2 and 4) and without (lanes 1 and 3) PNGase F. yEmCBP1 (lanes 1 and 2) and yEmCBP2 (lanes 3 and 4) were detected with alkaline phosphate-conjugated streptavidin. Molecular size markers are indicated on the left.

as humoral molecules and type I and type IV collagens and fibronectin as extracellular matrix molecules were chosen. All protein substrates used in this study were readily hydrolyzed by yEmCBP1 and yEmCBP2. All degradations of protein substrates were completely inhibited by adding a cysteine peptidase inhibitor, E-64 (data not shown).

4. Discussion

Numerous studies have demonstrated that cysteine peptidases from protozoa, trematode and nematode parasites are involved in various functions including nutrient uptake, disruption of the immune system, invasion and penetration into host tissues, which leads us strongly to consider them as a likely target for the chemotherapy (reviewed by Sajid and McKerrow, 2002; Dalton et al., 2003; Caffrey et al., 2004; Rosenthal, 2004; McKerrow et al., 2006; Robinson et al., 2008; Smooker et al., 2010). By contrast, few characterizations of peptidases including cysteine peptidases of cestodes *E. multilocularis* and *Echinococcus granulosus* have been described (McManus and Barrett, 1985; Marco and Nieto, 1991; Sako et al., 2007). In this study, two cathepsin B-like cysteine peptidases, EmCBP1 and EmCBP2, from *E. multilocularis* metacestode were identified, functionally expressed and characterized.

Sequencing analyses revealed that EmCBP1 and EmCBP2 have a catalytic triad (Cys, His, and Asn) and an oxyanion hole (Menard et al., 1991) those are characteristic features of clan CA family C1 cysteine peptidase. The occluding loop that is responsible for peptidyldipeptidase activity (Musil et al., 1991) and is a feature distinguishing cathepsin B from other cysteine peptidases is also conserved. RT-PCR analyses using EmCBP1 and EmCBP2-specific primer, in addition to the fact that EmCBP1 and EmCBP2 were found in the database of *E. multilocularis* whole genome project (http://www.sanger.ac.uk/resources/downloads/helminths/echinococcus-multilocularis.html), demonstrated that the genes obtained were originated from *E. multilocularis*, not from mouse used for preparation of parasite materials (data not shown).

Immunoblot and immunohistochemical experiments demonstrated that EmCBP1 and EmCBP2 were expressed in the germinal layer, the brood capsule and the protoscolex of larva and that some portions of both enzymes were secreted. The sizes, 24.5 and 25.5 kDa, of proteins detected by anti-EmCBP1 monoclonal antibody were smaller than the predicted size, 28.4 kDa. Cathepsin B is synthesized as an inactive 43 kDa pro-form and is processed to a single-chain form (31 kDa) or a two-chain form (heavy chain of 25 kDa and light chain of 5 kDa) to be activated (Towatari et al., 1979). It is possible that EmCBP1 consists of a heavy chain and light chain linking by a disulphide bond, and the protein bands detected by monoclonal antibody might be derived from the heavy chains. Anti-EmCBP2 monoclonal antibody recognized protein of 27.0 and 29.9 kDa in lysate and ES products. The latter protein might be intermediate forms of proenzyme. Determinations of N-terminal amino acid sequences of purified native EmCBP1 and EmCBP2 must be carried out.

The expressions of the active recombinant EmCBP1 and EmCBP2 were conducted by the use of the *P. pastoris* expression system. yEmCBP1 was successfully activated at pH 4.5 and purified. Because of the existence of one N-glycosylation site in mature enzyme, yEmCBP1 was glycosylated and detected as a broad band with 25–50 kDa range in size after purification. Some portion of yEmCBP1, detected as a 25.6 kDa-protein by immunoblot analysis after treated with PNGase F, could not be labelled efficiently with active enzyme-specific probe, biotin-Phe-Ala-FMK, which indi-

Please cite this article in press as: Sako, Y., et al. *Echinococcus multilocularis*: Identification and functional characterization of cathepsin B-like peptidases from metacestode. Exp. Parasitol. (2010), doi:10.1016/j.exppara.2010.11.005

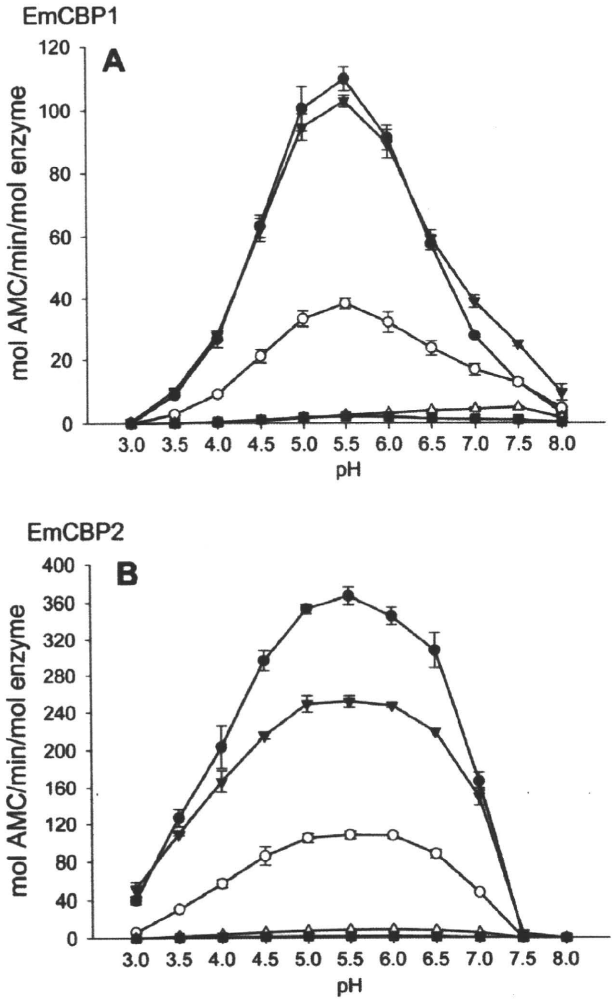

Fig. 5. pH optima and S2 subsite specificity of yEmCBP1 and yEmCBP2. Five substrates, Z-Phe-Arg-MCA (closed circles), Z-Val-Val-Arg-MCA (closed triangles), Z-Leu-Arg-MCA (open circles), Z-Gly-Pro-Arg-MCA (closed squares), and Z-Arg-Arg-MCA (open triangles) were tested at a final concentration of 2 μM. The standard deviation of three experiments is indicated.

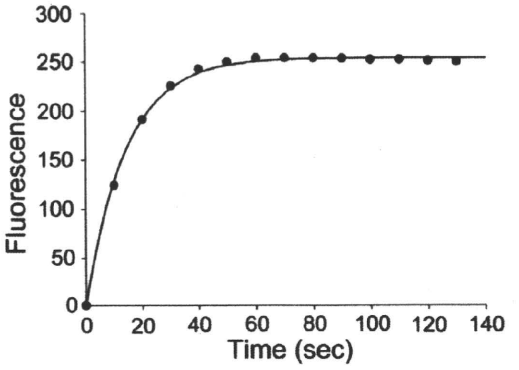

Fig. 6. Progress curve for the inactivation of yEmCBP2 at pH 7.5. Substrate, Z-Phe-Arg-MCA, was tested at a final concentration of 50 μM, and progress of the reaction was monitored continuously by the fluorescence of the released products. The solid line is the theoretical first-order curve calculated using Eq. 1.

Table 2
Effect of pH on the rate of inactivation of yEmCBP1 and yEmCBP2.[a]

	pH	$10^3 \times k_{obs}$ (s^{-1})	$t_{1/2}$ (s)
yEmCBP1	6.5	Nob[b]	Nob
	7.0	Nob	Nob
	7.5	2.18 ± 0.02	317.69 ± 3.40
yEmCBP2	6.5	0.41 ± 0.01	1689.29 ± 61.11
	7.0	6.79 ± 0.48	102.32 ± 7.20
	7.5	70.52 ± 2.23	9.83 ± 0.31

[a] The best estimates for the observed inactivation rate constant, k_{obs}, are given by nonlinear regression analysis. Corresponding half-lives were calculated using following relation ship: $t_{1/2} = \ln 2/k_{obs}$. Inactivation was investigated in the presence of 50 μM Z-Phe-Arg-MCA.

[b] Nob = not observed during incubation.

cated that they were inactive enzyme. This may be due to miss-folding, the oxidation, or the autodegradation of the mature enzyme during expression and purification. Activation of yEmBP2 was unsuccessful under the same condition of yEmCBP1 activation. Alternative activation condition in the presence of negatively charged glycosaminoglycan with dextran sulfate which facilitates autocatalytic activation (Barlic-Maganja et al., 1998) was tested but resulted in unsuccessful (data not shown). However, active yEmCBP2 could be obtained by *trans*-processing with pepsin, resulting in a single 27 kDa-protein.

In cysteine peptidases belonging to clan CA, the S2 subsite is substantial substrate-binding pocket for determination of substrate specificity (McGrath, 1999). The substrate specificity of the yEmCBP1 and yEmCBP2 was characterized by the use of several peptide substrates varying at P2 position. Both enzymes preferred substrates with Phe > Val > Leu at P2 position at an acidic pH optimum of 5.5, and cathepsin B-selective substrate Z-Arg-Arg-MCA was less hydrolyzed. Kinetic parameters for hydrolysis of Z-Phe-Arg-MCA and Z-Arg-Arg-MCA revealed that there were 93- and 137-fold-differences in k_{cat}/K_m values for yEmCBP1 and yEmCBP2, respectively. Similar preference has been observed in a cathepsin B isoform (SmCB2) of *Schistosoma mansoni*, not other isoform (SmCB1) (Caffrey et al., 2002). By contrast, the difference reported for mammalian cathepsin B is smaller than 10-fold (Hasnain et al., 1992; Wang et al., 1998). EmCBP1, EmCBP2 and SmCB2 have a negatively charged residue Asp at position 173 (mouse cathepsin B

Table 1
Kinetic parameters for hydrolysis of peptidyl-MCA substrates by yEmCBP1 and yEmCBP2.[a]

	Substrate	K_m (μM)	k_{cat} (s^{-1})	k_{cat}/K_m ($mM^{-1}\ s^{-1}$)
yEmCBP1	Z-Phe-Arg-MCA	20.45 ± 1.23	33.23 ± 1.01	1626.71 ± 48.67
	Z-Arg-Arg-MCA	747.67 ± 41.15	13.05 ± 0.63	17.46 ± 0.11
yEmCBP2	Z-Phe-Arg-MCA	27.17 ± 0.82	71.68 ± 1.52	2638.40 ± 23.29
	Z-Arg-Arg-MCA	1124.47 ± 76.15	21.57 ± 1.05	19.19 ± 0.36

[a] The K_m and V_{max} values were calculated by a nonlinear regression analysis of substrate concentration versus peptidase velocity. The k_{cat} values were calculated from V_{max} and the molar concentration of active enzyme titrated with Z-Phe-Arg-MCA and cysteine peptidase inhibitor E-64.

Please cite this article in press as: Sako, Y., et al. *Echinococcus multilocularis*: Identification and functional characterization of cathepsin B-like peptidases from metacestode. Exp. Parasitol. (2010), doi:10.1016/j.exppara.2010.11.005

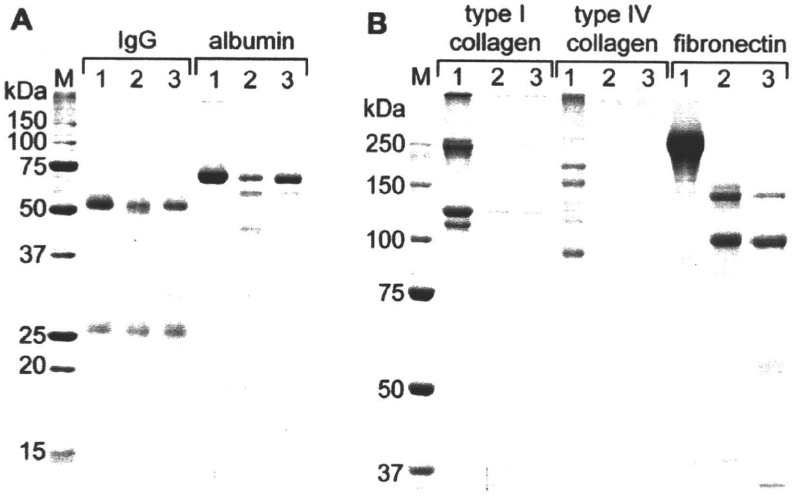

Fig. 7. Degradation of macromolecules by yEmCBP1 and yEmCBP2. Humoral molecules (A) and extracellular matrix molecules (B) were incubated with yEmCBP1 or yEmCBP2 at 37 °C for 4 h at pH 5.5. Protein substrate digests were subjected to SDS–PAGE and degradation products were visualized by Coomassie Blue staining. Each substrate was incubated with none of enzyme (lanes 1), yEmCBP1 (lanes 2), and yEmCBP2 (lanes 3). Molecular size markers are indicated on the left.

numbering) involving in S2 subsite formation, whereas mammalian cathepsin B from human, mouse, rat, and bovine and SmCB1 have an uncharged residue, Ala and Ser, respectively, without other substantial differences. Therefore, the possibility that the negatively charged residue Asp participates in the substrate preference is raised. Further analyses by using recombinant enzymes in which Asp is replaced with Ala are necessary to confirm this possibility.

The facts that at acidic condition yEmCBP1 and yEmCBP2 were stable, active and had broad specificity against host proteins including immunoglobulin, albumin, collagens, and fibronectin, suggested that these enzymes are lysosomal enzymes and are involved in protein digestion for parasites' nutrition. Additionally, the possibility that yEmCBP1 and yEmCBP2 act as extracellular enzymes was raised since both enzymes were detected in ES products. However, yEmCBP1 and yEmCBP2, especially latter, were unstable at neutral or slightly alkaline pH close to physiological pH similarly to mammal papain-like cysteine peptidases except for cathepsin S (Turk et al., 2000). Since the echinococcal cyst fluid has a neutral pH, EmCBP1 and EmCBP2 secreted into cyst fluid might lose their enzymatic activity. In contrast, EmCBP1 and EmCBP2 secreted outside of parasite cysts might not lose their enzymatic activity, because it is known that the host inflammatory responses can lead to tissue acidification (Kellum et al., 2004) and cathepsin B secreted from some kind of tumor cells becomes stable at alkaline pH by interacting with heparin and heparan sulfate (Almeida et al., 2001; Roshy et al., 2003). The activities of cysteine peptidases secreted into host tissues to degrade extracellular matrix molecules, e.g., collagen and fibronectin, have been described in several nematode and trematode parasites (Berasain et al., 1997; Rhoads and Fetterer, 1997; Smooker et al., 2010), and these characters seem to be implicated in migration of parasite through host tissues. Because the larva of *E. multilocularis* infiltrates and proliferates indefinitely by exogenous budding of the cellular germinal layer (Thompson, 1995), the ability of EmCBP1 and EmCBP2 to degrade extracellular matrix molecules might be involved in pathogenesis of *E. multilocularis*. Inhibition analyses of EmCBP1 and EmCBP2 by specific inhibitors or genetic knock out of enzymes would be needed to confirm such a role of peptidases *in vivo*.

In conclusion, we identified and characterized two novel cathepsin B-like peptidases from *E. multilocularis* metacestodes. The enzymes may play a primary role in protein digestion for parasites' nutrition. Thus, the inactivation of these enzymes may impair the survival of the parasite in the host. Further studies are needed to provide a greater understanding of the biological significance of EmCBP1 and EmCBP2 in parasite–host interactions.

Acknowledgements

This study was supported in part by the Japan Society for the Promotion of Science (JSPS) (21256003), JSPS-Asia/Africa Science Platform Fund (2006–2011) and by the Special Coordination Fund for Promoting Science & Technology (2010–2012) by Ministry of Education, Japan.

References

Abdulla, M.H., Lim, K.C., Sajid, M., McKerrow, J.H., Caffrey, C.R., 2007. Schistosomiasis mansoni: novel chemotherapy using a cysteine protease inhibitor. PLoS Medicine 4, e14.

Alcala-Canto, Y., Ibarra-Velarde, F., Sumano-Lopez, H., Gracia-Mora, J., Alberti-Navarro, A., 2007. Effect of a cysteine protease inhibitor on *Fasciola hepatica* (liver fluke) fecundity, egg viability, parasite burden, and size in experimentally infected sheep. Parasitology Research 100, 461–465.

Almeida, P.C., Nantes, I.L., Chagas, J.R., Rizzi, C.C., Faljoni-Alario, A., Carmona, E., Juliano, L., Nader, H.B., Tersariol, I.L., 2001. Cathepsin B activity regulation. Heparin-like glycosaminogylcans protect human cathepsin B from alkaline pH-induced inactivation. The Journal of Biological Chemistry 276, 944–951.

Barlic-Maganja, D., Dolinar, M., Turk, V., 1998. The influence of Ala205 on the specificity of cathepsin L produced by dextran sulfate assisted activation of the recombinant proenzyme. Biological Chemistry 379, 1449–1452.

Barr, S.C., Warner, K.L., Kornreic, B.G., Piscitelli, J., Wolfe, A., Benet, L., McKerrow, J.H., 2005. A cysteine protease inhibitor protects dogs from cardiac damage during infection by *Trypanosoma cruzi*. Antimicrobial Agents and Chemotherapy 49, 5160–5161.

Berasain, P., Goni, F., McGonigle, S., Dowd, A., Dalton, J.P., Frangione, B., Carmona, C., 1997. Proteinases secreted by *Fasciola hepatica* degrade extracellular matrix and basement membrane components. Journal of Parasitology 83, 1–5.

Barrett, A.J., Kirschke, H., 1981. Cathepsin B, Cathepsin H, and cathepsin L. Methods in Enzymology 80, 535–561.

Caffrey, C.R., McKerrow, J.H., Salter, J.P., Sajid, M., 2004. Blood 'n' guts: an update on schistosome digestive peptidases. Trends in Parasitology 20, 241–248.

Caffrey, C.R., Salter, J.P., Lucas, K.D., Khiem, D., Hsieh, I., Lim, K.C., Ruppel, A., McKerrow, J.H., Sajid, M., 2002. SmCB2, a novel tegumental cathepsin B from adult *Schistosoma mansoni*. Molecular and Biochemical Parasitology 121, 49–61.

Dalton, J.P., Neill, S.O., Stack, C., Collins, P., Walshe, A., Sekiya, M., Doyle, S., Mulcahy, G., Hoyle, D., Khaznadji, E., Moiré, N., Brennan, G., Mousley, A., Kreshchenko, N., Maule, A.G., Donnelly, S.M., 2003. *Fasciola hepatica* cathepsin L-like proteases: biology, function, and potential in the development of first generation liver fluke vaccines. International Journal for Parasitology 33, 1173–1181.

Eckert, J., Conraths, F.J., Tackmann, K., 2000. Echinococcosis: an emerging or re-emerging zoonosis? International Journal for Parasitology 30, 1283–1294.

Hasnain, S., Hirama, T., Tam, A., Mort, J.S., 1992. Characterization of recombinant rat cathepsin B and nonglycosylated mutants expressed in yeast. New insights into the pH dependence of cathepsin B-catalyzed hydrolyses. The Journal of Biological Chemistry 267, 4713–4721.

Please cite this article in press as: Sako, Y., et al. *Echinococcus multilocularis*: Identification and functional characterization of cathepsin B-like peptidases from metacestode. Exp. Parasitol. (2010), doi:10.1016/j.exppara.2010.11.005

Ito, A., Agvaandaram, G., Bat-Ochir, O.-E., Chuluunbaatar, B., Gonchigsenghe, N., Yanagida, T., Sako, Y., Myadagsuren, N., Dorjsuren, T., Nakaya, K., Nakao, M., Ishikawa, Y., Davaajav, A., Dulmaa, N., 2010. Histopathological, serological, and molecular confirmation of indigenous alveolar echinococcosis cases in Mongolia. American Journal of Tropical Medicine and Hygiene 82, 266–269.

Kellum, J.A., Song, M., Li, J., 2004. Science review: extracellular acidosis and the immune response: clinical and physiologic implications. Critical Care 8, 331–336.

Kern, P., 2006. Medical treatment of echinococcosis under the guidance of Good Clinical Practice (GCP/ICH). Parasitology International 55 Suppl, S273–S282.

Marco, M., Nieto, A., 1991. Metalloproteinases in the larvae of *Echinococcus granulosus*. International Journal for Parasitology 21, 743–746.

McGrath, M.E., 1999. The lysosomal cysteine proteases. Annual Review of Biophysics and Biomolecular Structure 28, 181–204.

McKerrow, J.H., Caffrey, C., Kelly, B., Loke, P., Sajid, M., 2006. Proteases in parasitic diseases. Annual Review of Pathology 1, 497–536.

McManus, D.P., Barrett, N.J., 1985. Isolation, fractionation and partial characterization of the tegumental surface from protoscoleces of the hydatid organism, *Echinococcus granulosus*. Parasitology 90, 111–129.

McManus, D.P., Zhang, W., Li, J., Bartley, P.B., 2003. Echinococcosis. Lancet 362, 1295–1304.

Menard, R., Carriere, J., Laflamme, P., Plouffe, C., Khouri, H.E., Vernet, T., Tessier, D.C., Thomas, D.Y., Storer, A.C., 1991. Contribution of the glutamine 19 side chain to transition-state stabilization in the oxyanion hole of papain. Biochemistry 30, 8924–8928.

Molinari, J.L., Mejia, H., White Jr., A.C., Garrido, E., Borgonio, V.M., Baig, S., Tato, P., 2000. *Taenia solium*: a cysteine protease secreted by metacestodes depletes human CD4 lymphocytes *in vitro*. Experimental Parasitology 94, 133–142.

Musil, D., Zucic, D., Turk, D., Engh, R.A., Mayr, I., Huber, R., Popovic, T., Turk, V., Towatari, T., Katunuma, N., Bode, W., 1991. The refined 2.15 A X-ray crystal structure of human liver cathepsin B: the structural basis for its specificity. The EMBO Journal 10, 2321–2330.

Nakaya, K., Mamuti, W., Xiao, N., Sato, M.O., Wandra, T., Nakao, M., Sako, Y., Yamasaki, H., Ishikawa, Y., Craig, P.S., Schantz, P.M., Ito, A., 2006. Usefulness of severe combined immunodeficiency (scid) and inbred mice for studies of cysticercosis and echinococcosis. Parasitology International 55 Suppl, S91–S97.

Nielsen, H., Engelbrecht, J., Brunak, S., von Heijne, G., 1997. Identification of prokaryotic and eukaryotic signal peptides and prediction of their cleavage sites. Protein Engineering 10, 1–6.

Pawlowski, Z.S., Eckert, J., Vuitton, D.A., Ammann, R.W., Kern, P., Craig, P.S., Far, K.F., De Rosa, F., Filice, C., Gottstein, B., Grimm, F., Macpherson, C.N.L., Sato, N., Todorov, Uchino, J., von Sinner, W., Wen, H., 2001. Echinococcosis in humans: clinical aspects, diagnosis and treatment. In: Eckert, J., Gemmell, M.A., Meslin, F.-X., Pawlowski, Z.S. (Eds.), WHO/OIE manual on echinococcosis in humans and animals: a public health problem of global concern. World Organization for Animal Health, Paris, France, pp. 20–71.

Rawlings, N.D., Tolle, D.P., Barrett, A.J., 2004. MEROPS: the peptidase database. Nucleic Acids Research 32, D160–D164.

Rhoads, M.L., Fetterer, R.H., 1997. Extracellular matrix: a tool for defining the extracorporeal function of parasite proteases. Parasitology Today 13, 119–122.

Robinson, M.W., Dalton, J.P., Donnelly, S., 2008. Helminth pathogen cathepsin proteases: it's a family affair. Trends in Biochemical Sciences 33, 601–608.

Rosenthal, P.J., 2004. Cysteine proteases of malaria parasites. International Journal for Parasitology 34, 1489–1499.

Roshy, S., Sloane, B.F., Moin, K., 2003. Pericellular cathepsin B and malignant progression. Cancer and Metastasis Reviews 22, 271–286.

Sajid, M., McKerrow, J.H., 2002. Cysteine proteases of parasitic organisms. Molecular and Biochemical Parasitology 120, 1–21.

Sako, Y., Yamasaki, H., Nakaya, K., Nakao, M., Ito, A., 2007. Cloning and characterization of cathepsin L-like peptidases of *Echinococcus multilocularis* metacestodes. Molecular and Biochemical Parasitology 154, 181–189.

Shin, M.H., Chung, Y.B., Kita, H., 2005. Degranulation of human eosinophils induced by *Paragonimus westermani*-secreted protease. Korean Journal of Parasitology 43, 33–37.

Smooker, P.M., Jayaraj, R., Pike, R.N., Spithill, T.W., 2010. Cathepsin B proteases of flukes: the key to facilitating parasite control? Trends in Parasitology 26, 506–514.

Tato, P., Fernández, A.M., Solano, S., Borgonio, V., Garrido, E., Sepúlveda, J., Molinari, J.L., 2004. A cysteine protease from *Taenia solium* metacestodes induce apoptosis in human CD4+ T-cells. Parasitology Research 92, 197–204.

Thompson, R.C.A., 1995. Biology and systematics of *Echinococcus*. In: Thompson, R.C.A., Lymbery, A.J. (Eds.), *Echinococcus* and Hydatid Disease. CAB International, Wallingford, UK, pp. 1–50.

Towatari, T., Kawabata, Y., Katunuma, N., 1979. Crystallization and properties of cathepsin B from rat liver. European Journal of Biochemistry 102, 279–289.

Turk, B., Turk, D., Turk, V., 2000. Lysosomal cysteine proteases: more than scavengers. Biochimica et Biophysica Acta 1477, 98–111.

Wang, B., Shi, G.P., Yao, P.M., Li, Z., Chapman, H.A., Bromme, D., 1998. Human cathepsin F. Molecular cloning, functional expression, tissue localization, and enzymatic characterization. The Journal of Biological Chemistry 273, 32000–32008.

Please cite this article in press as: Sako, Y., et al. *Echinococcus multilocularis*: Identification and functional characterization of cathepsin B-like peptidases from metacestode. Exp. Parasitol. (2010), doi:10.1016/j.exppara.2010.11.005

CHAPTER 51

Cysticercosis and taeniosis: *Taenia solium, Taenia saginata* and *Taenia asiatica*

Ana Flisser, Philip S. Craig and Akira Ito

Summary

The pork and beef tapeworms, *Taenia solium* and *Taenia saginata* respectively, are taeniid cestodes and major food-borne or meat-borne zoonoses. Human tapeworms and swine cysticerci have been known since Egyptian and Greek cultures. Nevertheless their association as part of the life cycle of the same parasite was only demonstrated during the nineteenth century. Kuchenmeister fed convicts with cysticerci excised from pork meat and found adult tapeworms in the intestine after autopsy, while van Beneden fed *T. solium* eggs to pigs and found numerous cysticerci in muscles after slaughter (Grove 1990).

T. solium is the only causative agent of neurocysticercosis in humans and is, therefore, the more important of these species in public health. This chapter describes classical aspects of the morphology of the parasites as well as clinical aspects of the diseases they cause. Most importantly, detailed explanations of taxonomic aspects, specially related to the newly recognized *Taenia asiatica* are given. Furthermore, the epidemiology and transmission dynamics of the parasites, as well as intervention measures such as health education, mass drug treatment and vaccination, are described in detail. The chapter concludes with considerations on the surveillance and a discussion on prospects for the control of these cestode zoonoses.

Taxonomy

The classification of human *Taenia* is as follows:

Kingdom: Animalia,

Phylum: Platyhelminthes,

Class: Cestoidea,

Subclass: Eucestoda,

Order: Cyclophyllidea,

Family: Taeniidae,

Genus: *Taenia*,

Species: *Taenia solium* Linnaeus (1758),

Species: *Taenia saginata* Goeze (1782),

Species: *Taenia asiatica* Eom and Rim (1993).

Taeniidae are mammalian parasites with adults found in carnivores and larvae in herbivores. In the adult parasite, the scolex, which is the anchorage organ aided by suckers, usually bears 2 rows of hooks that rarely are absent. The genital pore is irregularly alternated along the strobila with a single set of reproductive organs in each proglottid. Eggs have a radial striated appearance because of the embryophore formed by embryophoric blocks.

Adult *Taenia solium* and *Taenia saginata* are found in the human intestine. The larval stage or metacestode (cysticercus) is found in pigs (*T. solium*) and bovines (*T. saginata*).

Taenia asiatica has been recognized in Asia and the Pacific. Adult tapeworms appear to be *T. saginata* but infected people eat pork rather than beef (Huang *et al.* 1966; Kosin *et al.* 1972; Fan 1988). It has been called the Asian *Taenia* and expected to be a new species (Fan 1988; reviewed by Simanjuntak *et al.* 1997). Subsequent molecular studies revealed very small differences from *T. saginata* and it was classified as a subspecies of *T. saginata* (*T. saginata asiatica*, Fan *et al.* 1995), which used different intermediate hosts distributed in Asia and the Pacific (Fan 1988, 1995; McManus and Bowles 1994). Later, it was described as *Taenia asiatica*, an independent but sister species of *T. saginata* (reviewed by Ito *et al.* 2003; Eom 2006; Hoberg 2006). Separate species are believed to be valid as *T. saginata* and *T asiatica* are distribute sympatrically but to data no hybrids between the two have been identified which would be expected if they were subspecies or strains of the same species. However, the numbers of specimens to date examined is small. (Hoberg 2006). Fig. 51.1 illustrates a summary of the molecular phylogeny of taeniid cestodes (modified from Okamoto *et al.* 2007).

Molecular phylogeny

Molecular tools have been used to further characterize the 3 human *Taenia* species (McManus and Ito 2005) and their epidemiology and possible origin. Mitochondrial DNA data strongly suggest that *T. saginata* and *T. asiatica* are very closely related to each other and

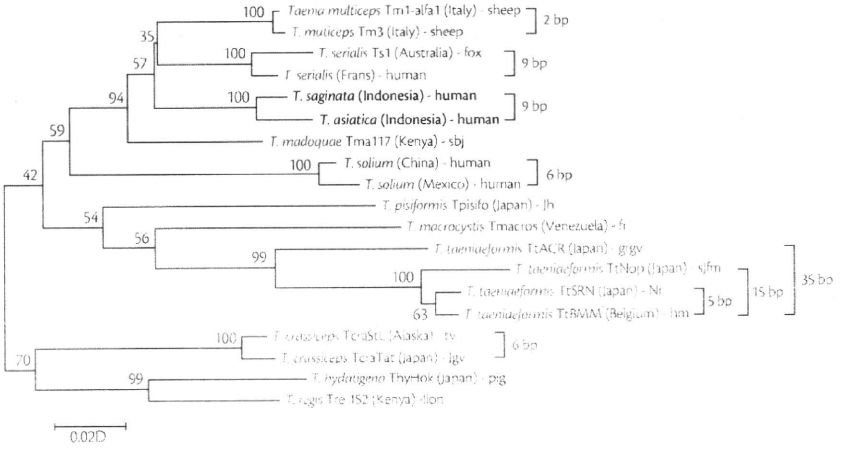

Fig. 51.1 Molecular phylogeny of genus *Taenia*.
Modified from Okamoto et al. (2007).

that *T. solium* is divided into two genotypes, the Asian and the American/African genotypes (Fig. 51.2). Minor diversity within the genotypes has been demonstrated in samples from Peru and Mexico (Nakao *et al.* 2002; Campbell *et al.* 2006; Maravilla *et al.* 2003, 2008; Sudewi *et al.* 2008). Molecular phylogenic studies (Sudewi *et al.* 2008) suggest that *T. solium* in Papua originated elsewhere in Asia rather than from nearby Bali as suggested by Gadjusek (1978).

T. saginata mitochondrial DNA analysis shows large variations (Rodriguez-Hidalgo *et al.* 2002; Myadagsuren *et al.* 2007) pointing to a higher complexity of this parasite than that of *T. solium*.

T. solium emerged in Africa several millions years ago as a parasite of early hominids that probably evolved from parasites of hyaeniids (Hoberg 2001, 2006).

Detection of parasite DNA using faecal samples and multiplex PCR for identification of human *Taenia* should be used in endemic areas for *T. solium*, *T. saginata* and *T. asiatica*, because their sympatric distribution may complicate surveillance of cysticercosis control (Ananthaphruti *et al.* 2007).

Morphology

Tapeworm

Tapeworms are flat long helminths: adults measuring 1.5 to 10 m. The head or scolex, has four suckers and a rostellum, which may be armed with hooks (*T. solium*), unarmed (*T. saginata*) or have a sunken or unarmed rostellum (*T. asiatica*, Fig. 51.3). Hooks are organized as a two row crown of 22 to 32 hooks that ranges in size from 159 to 173 µm. The most conspicuous part of the tapeworm is the chain of segments that forms the strobila. It has the appearance of a ribbon and is constituted by more than a thousand proglottids (proper name for segments). Tapeworms do not have digestive organs, thus feed passively through their tegument. In contrast they have a well formed excretory system that contains numerous collecting ducts and flame cells. Proglottids develop from the neck region behind the scolex. Proximal proglottids are immature, they are followed by mature ones that contain several

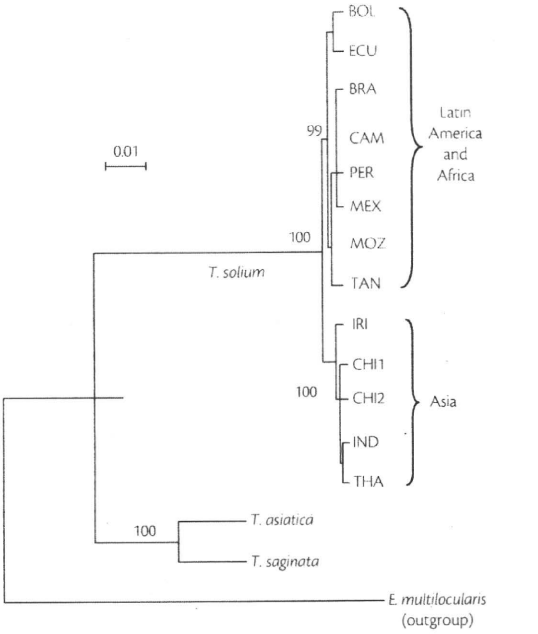

Fig. 51.2 Two genotypes of *T. solium* in the world. The neighbour-joining phylogenetic tree of taeniid tapeworms inferred from the complete nucleotide sequences of mitochondrial *cox1* gene. The scale bar represents the estimated number of nucleotide substitutions per nucleotide site. The isolates of *T. solium* were obtained from Bolivia (BOL), Ecuador (ECU), Brazil (BRA), Cameroon (CAM), Peru (PER), Mexico (MEX), Mozambique (MOZ), Tanzania (TAN), Irian Jaya (IRI), China (CHI1 and CHI2), India (IND) and Thailand (THA).
Modified from Nakao *et al.* (2002).